ELSEVIER

#### Contents lists available at ScienceDirect

# Journal of Hydrology

journal homepage: www.elsevier.com/locate/jhydrol



#### Research papers

# The role of spatiotemporal plant trait variability in model predictions of ecohydrological responses to climate change in a desert shrubland



Shaoqing Liu<sup>a,\*</sup>, Gene-Hua Crystal Ng<sup>a,b</sup>

- a Department of Earth Sciences, University of Minnesota, Twin Cities, Minneapolis, MN, USA
- <sup>b</sup> Saint Anthony Falls Laboratory, University of Minnesota, Twin Cities, Minneapolis, MN, USA

#### ARTICLE INFO

This manuscript was handled by G. Syme, Editor-in-Chief

Keywords: Ecohydrological model Plant functional trait Model-data fusion

#### ABSTRACT

Although spatial heterogeneity of soil properties, topography, and climate is commonly incorporated into ecohydrological models, the spatial and temporal variability in plant functional traits is typically overlooked. The objective of our study is to evaluate the impact of trait parameter variability on modeled ecohydrological processes. We implemented a model-data fusion approach to constrain spatiotemporally dynamic parameters in plant functional traits at two desert shrubland sites located along a topographic and climate gradient in the Mojave Desert. Our results showed that the estimates for specific leaf area and rooting depth for the broadleafevergreen-shrub plant-functional-type showed spatial variability, with lower specific leaf area and deeper rooting depth found at the low elevation site. We also found that the specific leaf area estimates changed over time at both sites in response to water stress, but with different sensitivities, possibly depending on species and/ or climate. The spatial variability in trait parameter estimates was greater than temporal variability and played a more important role in accurately simulating ecohydrological processes, but including the temporal variability in specific leaf area further improved seasonal predictions. In simulations forced by future climate projections under the Representative Concentration Pathway 4.5 (RCP 4.5) and 8.5 (RCP 8.5) greenhouse gas emissions scenarios, spatial variability in trait parameters impacted predictions of both carbon and water fluxes, while temporal variability in trait parameters resulted in predictions of higher ecological function and water use efficiency. The higher water use efficiency led to improved ecohydrological function in simulations under RCP 4.5, but it showed little capacity for buffering intensive water stresses under the more pessimistic RCP 8.5 scenario, indicating that with spatiotemporally variable trait parameters, the impact on predicted ecohydrological processes depends on the climate projections. Overall, our modeling results prompt further field-based examination of temporal and belowground trait variability in desert shrublands, and they raise the question of how combined spatiotemporal variabilities of multiple traits may support ecohydrological function under water stress.

## 1. Introduction

Ecological and hydrological processes are strongly coupled through complex biophysical and biogeochemical functions at multiple spatial and temporal scales, and this coupling is critical for understanding ecosystem resilience and vulnerability (Rodriguez-Iturbe et al., 1999; Wagener et al., 2010). On the one hand, water flow drives and controls plant physiological properties and plant community composition and distribution. On the other hand, vegetation plays a key role in regulating the water cycle through canopy interception, transpiration, and influence on surface properties (Chapin et al., 2002). Ecohydrological models have been developed to describe the coupled interactions between vegetation dynamics and hydrological processes (Rodriguez-

Iturbe, 2000; Chen et al., 2015). In addition to abiotic hydrological processes, these models incorporate vegetation modules to describe biophysical processes (canopy interception and evapotranspiration) (e.g., Abbott et al., 1986; Wigmosta et al., 1994; Liang et al., 1994), and some also represent plant biochemical processes (e.g., photosynthetic fluxes), physiological growth (e.g., changes in leaf area index), and dynamic changes in plant-type distribution (e.g. Band et al., 1993).

Previous ecohydrological investigations reveal that plant-water interactions exhibit spatiotemporal heterogeneity due to variability in climate, terrain, and vegetation type (Grayson et al., 1997; Mohanty and Skaggs, 2001; Waring and Running, 2010). To address this, most ecohydrological model implementations take in spatially distributed inputs of meteorological time series, soil hydraulic parameters, and

E-mail address: sqliu@umn.edu (S. Liu).

<sup>\*</sup> Corresponding author.

vegetation properties (e.g. Band et al., 1993; Wigmosta et al., 1994; Oleson et al., 2010). For representing vegetation properties, a major complication is the daunting number of vegetation species globally (Alton, 2011). To help make the problem more tractable, the concept of plant functional types (PFTs) was developed to represent main ecosystems (e.g. Oleson and Bonan, 2000; Bonan et al., 2002). Different model grid cells can be assigned different PFTs, and in more process-based models, the different grid cells can have different simulated carbon fluxes and states (e.g., vegetation carbon stock) that change over time. The major simplification is that all species assigned to a particular PFT are assumed to share the same, static set of plant parameters over time to represent plant functional traits, which are key characteristics controlling plant growth, reproduction, and survival under different environmental conditions (van Kleunen and Fischer, 2007).

While convenient, this PFT-based modeling approach ignores observations that environmental variations may cause trait variations within one PFT that can be even larger than average trait differences between PFTs (Kattge et al., 2011). Aboveground functional traits have been found to vary spatially in correlation with temperature (Reich and Oleksyn, 2004), radiation (Niinemets 2007; Serbin et al., 2014), and rainfall (Castro-Díez et al., 1997; Schulze et al., 2006; Gouveia and Freitas, 2009; Gotsch et al., 2010; Mclean et al., 2014). Belowground trait variability is less well-studied compared to aboveground traits, but a few studies also report strong interactions between belowground traits (e.g. root traits) and spatially variable temperature (Zadworny et al., 2016) and water availability (Schenk and Jackson, 2002). Although less extensively documented than spatial trait variability, temporal trait variability can be comparable in magnitude (Serbin et al., 2014), and it has been found to represent a "plasticity" that reflects adaptations and evolution in response to environmental changes. A clear example is seasonal or drought-driven phenology, which directly causes temporal changes in physiological (e.g. photosynthetic capacity) (Grassi et al., 2005; Muraoka et al., 2010), morphological (e.g. leaf thickness) (Fullana-Pericàs et al., 2017), and phenological (e.g. flowering time) traits (Belanger et al., 1995; Zhang et al., 2007; Yang et al., 2016). Major trends in leaf phenology are captured to some degree in most ecohydrological models, but most other plant traits are represented by temporally constant parameters. This ignores findings that plants can also adapt to seasonal drought by modifying root characteristics (e.g. root depth; Marron et al., 2002), the carbon allocation scheme (e.g. root to shoot ratio; Smirnoff, 1998), and leaf morphological structure (e.g. specific leaf area; Nouvellon et al., 2010) - changes that can result in slower growth rate but improved water use efficiency. Over longer time periods, functional trait plasticity may also acclimate to temperature change (Smith and Dukes, 2013) and resources limitation (Reich et al., 2014).

Despite the growing recognition of plant trait variability, it is still unclear to what degree current constant-parameter PFT-based models are biased in their simulations of ecohydrological processes, nor how these biases may affect our ability to predict future changes in coupled carbon and water cycles. Some recent studies explicitly incorporated spatial trait variability into ecohydrological models using statistical methods (Verheijen et al., 2013; Ali et al., 2015; Butler et al., 2017), and they demonstrated that model simulations were sensitive to trait variability. However, much remains unknown about the drivers of trait variability: correlations between trait variability and climatic variables are relatively weak (Wright et al., 2005; Moles et al., 2014; Šímová et al., 2018). Focusing on under-characterized temporal trait variability, previous work by Liu and Ng (2019) presented a new framework for constraining temporally dynamic trait parameters. In an implementation of a Mojave Desert shrubland site, they found estimates of the leaf trait parameter specific-leaf-area (SLA) to be temporally dynamic in response to water availability, allowing greater simulated water use efficiency than with a temporally constant parameter. Prompted by this finding that temporal trait parameter variability could impact simulations of coupled plant-water conditions (as represented

by water use efficiency), the current study builds upon that work with the goal of evaluating how different characteristics of trait variability – spatial versus temporal – may affect ecohydrological process simulations, and whether these variabilities could have implications for predicting ecohydrological vulnerability or resilience of desert shrublands with models. Focusing on two study sites spanning a climate and terrain gradient in a Mojave Desert watershed, we applied a model-data fusion approach (Raupach et al., 2005; Liu and Gupta, 2007) to address the following questions: (1) How do the spatial and temporal variability in estimated trait parameters compare in this watershed? (2) Which type of trait variability - spatial versus temporal - plays a more important role in accurately simulating ecohydrological processes? (3) How does the spatiotemporal variability in trait parameters affect our predictions of ecosystem response to future climatic change?

#### 2. Method

#### 2.1. Overview

To investigate how spatial and temporal variability in plant trait parameters affects simulated ecohydrological fluxes and states, we conducted three model-data fusion experiments that statistically use observations to estimate model parameters and their uncertainties for two sites along a topographic and climate gradient in the Mojave Desert. The first experiment ("E1") followed the standard constant parameterization approach, in which all functional traits shared identical plant parameter values within one PFT. Correspondingly, a modeldata fusion approach was applied where observations from the two sites were used to estimate a single set of plant trait parameters that applied identically to both locations. In contrast, the second experiment ("E2") acknowledged that there could be spatial differences in plant trait parameters between the two sites. In this experiment, the model-data fusion framework was implemented separately at each of two different study sites to generate different plant estimates at each location. The third experiment ("E3") further allowed trait parameters to have temporal variability. It used the previously developed stochastic modeldata fusion approach from Liu and Ng (2019) to constrain potential temporal patterns in plant trait parameters at each of the two study sites. A schematic flow chart depicting the three parameterization experiments is shown in Fig. 1. We then simulated the ecohydrological fluxes and states for the two sites under future climate projections from the Representative Concentration Pathway 4.5 (RCP 4.5) and 8.5 (RCP 8.5) greenhouse gas (GHG) emissions scenarios (van Vuuren et al., 2011) using the parameter estimates derived from the three experiments.

#### 2.2. Study sites

With the strong link between plant function and water availability and less complexity in vegetation composition, desert shrublands are relatively ideal for investigating spatiotemporal variability in trait parameters and their response to environmental stressors. We selected two desert shrubland sites, "Kelmet" (860 m.a.s.l.) and "Globe" (1250 m.a.s.l.), located at a distance of 13 km from each other in Kelso Valley in the Mojave National Preserve, southeastern California, USA (Fig. 2a). As the two sites have different climatic and geological conditions as well as similar vegetation types but distinct species composition, they enable us to test our hypothesis that in response to environmental changes, plant functional traits within a PFT may exhibit spatiotemporal variability, and that these should be represented in ecohydrological models. Detailed information about the Kelmet site, as well as a description of previous work in Kelso Valley, can be found in Liu and Ng (2019). The Globe site was instrumented with a Hobo weather station (Onset Computer Corporation, Bourne, MA) that provided hourly precipitation, air temperature, and relative humidity measurements from 2005 through 2010. The model also requires solar

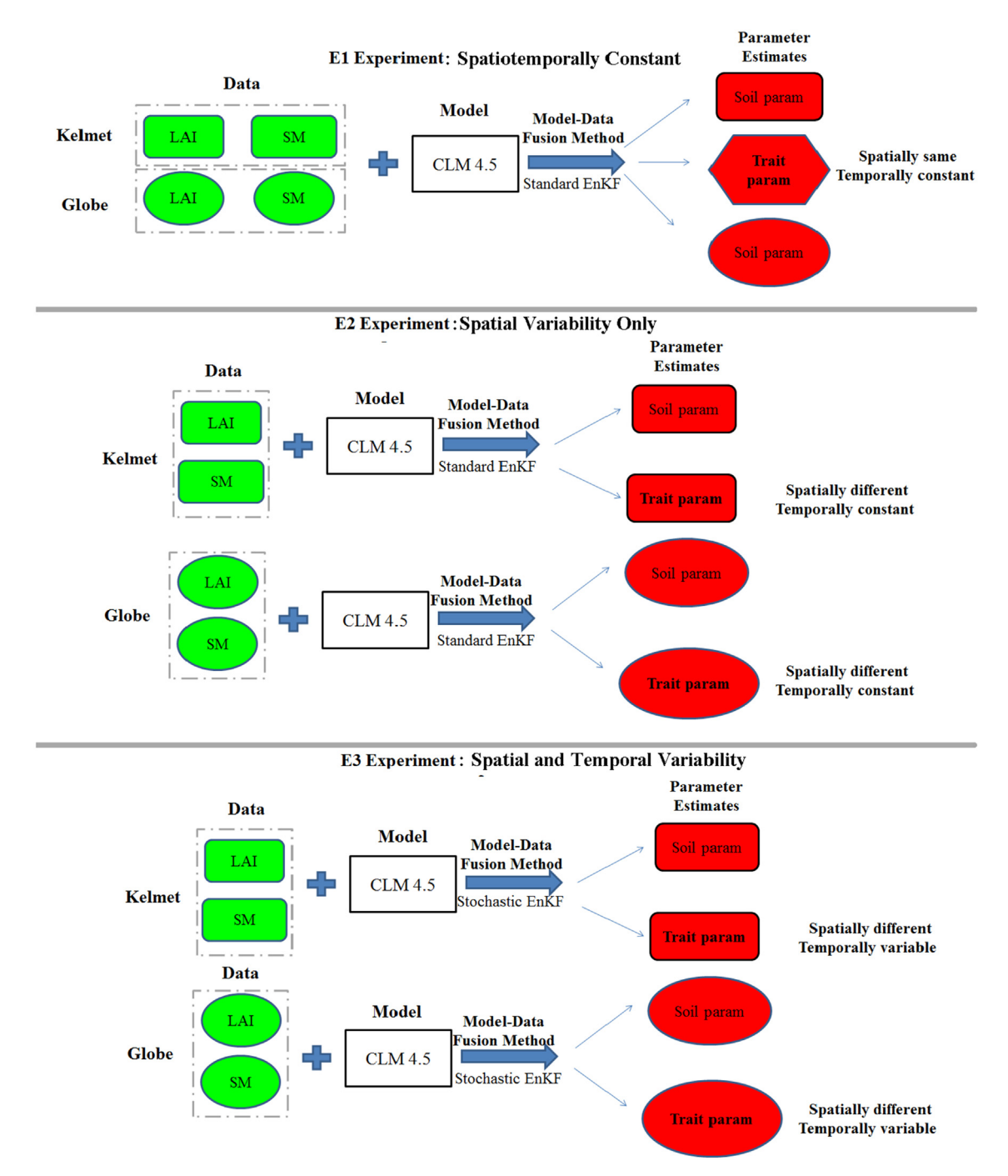


Fig. 1. Schematic flow chart for the three parameterization experiments. Calibration data include leaf area index ("LAI") and soil moisture ("SM") at the Kelmet site (indicated with rounded rectangles) and the Globe site (indicated with ovals). The Model-Data Fusion method is carried out using different implementations of the Ensemble Kalman Filter ("EnKF") with the CLM 4.5 ecohydrological model. Outputs include estimates of soil and plant trait parameters ("param").

radiation, wind speed, and air pressure data; these were taken from Kelmet, the closest fully instrumented location, with solar radiation values decreased by  $50~\text{W/m}^2$  when precipitation occurred at Globe but not Kelmet. To generate a longer meteorological time series that is representative of Globe, we extended the record back to 1 January 1961 using regional data (see Section S1 in Supplementary Information for details), similar to the reconstruction approach for Kelmet (Liu and Ng 2019).

In Kelso Valley, prominent rainfall occurs in the winter season with occasional convective storms in the summer. Reconstructed meteorological forcing time series from 1961 to 2010 indicate that the higher elevation Globe site is cooler and wetter (annual average temperature:

18.4 °C and precipitation: 291 mm/year) than the lower elevation Kelmet site (annual average temperature: 20.1 °C and precipitation: 103 mm/year) (Fig. 2b). Also, younger, coarser, and more homogeneous soils are present at the lower elevation Kelmet site compared to the Globe site (Miller et al., 2009). At the Kelmet site, 15% of the ground is covered by the broadleaf evergreen shrub *Larrea tridentata*, with the co-dominant drought-deciduous shrub *Ambrosia dumosa*, covering about 5%. Vegetation at the Globe site is more diverse, with *Prunus fasciculata* and *Ambrosia eriocentra* as the major shrubs present (see Section S2 in Supplementary Information for more details); overall, the broadleaf-evergreen-shrub and broadleaf-deciduous-shrub PFTs cover about 8% and 12% of the ground at Globe, respectively. Although

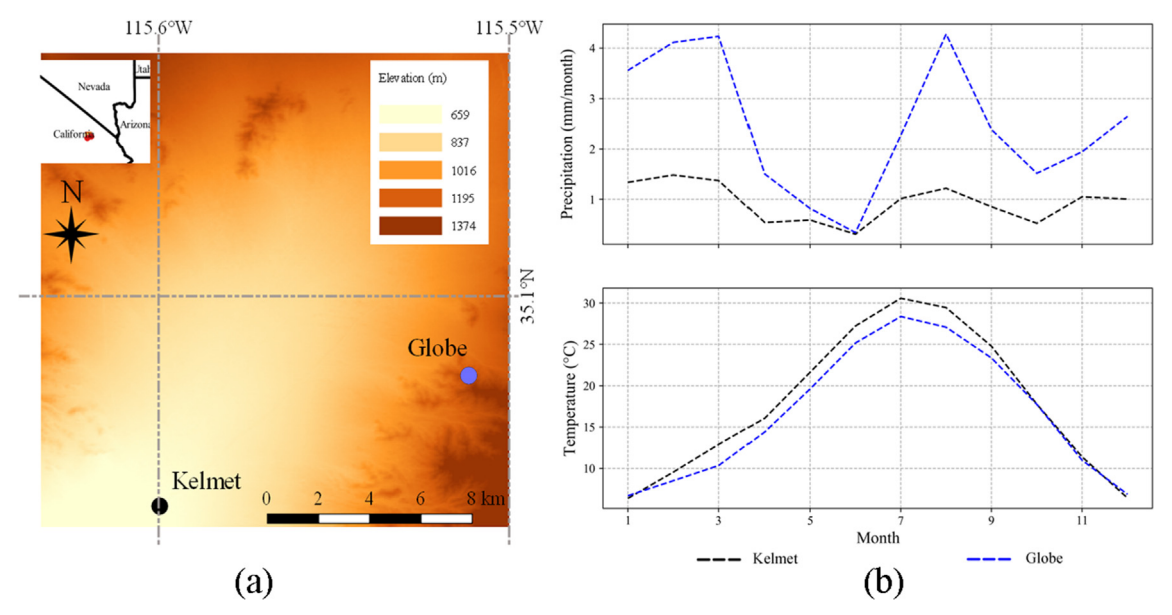


Fig. 2. Study sites in the Mojave Desert watershed (a); right figures shows the monthly mean precipitation and temperature from 1961 to 2010 at the Kelmet (lower elevation) and Globe (higher elevation) sites (b).

the plant species are different between the sites, most are categorized as broadleaf evergreen shrub or broadleaf deciduous shrub PFTs. This means that under the current PFT-based model paradigm, identical broadleaf evergreen shrub and broadleaf deciduous shrub parameters would be used for the two sites. In this study, we examine whether plant trait parameter estimates exhibit spatiotemporal variability at the two sites that affect ecohydrological process predictions. To use as model constraints on plant trait and soil hydraulic parameter estimates, soil moisture at 15 and 35 cm soil depths were measured at both sites from 2 July 2007 to 31 December 2010 using Hobo soil moisture probes (Onset Computer Corporation, Bourne, MA) (Kelmet observations were described in Ng et al., 2015), and 1-km, 8-day resolution leaf area index (LAI, ratio of the total surface area of all leaves to the ground area below) retrieval from Moderate Resolution Imaging Spectroradiometer (MODIS) (Myneni et al., 2002) were compiled over that period at both sites.

#### 2.3. Ecoyhdrological model

We used the Community Land Model version 4.5 (CLM4.5) (Oleson et al., 2010) to simulate coupled soil moisture and leaf area index (LAI, ratio of the total surface area of all leaves to the ground area below). CLM4.5 consists of multiple land surface processes including surface radiation transfer, energy/water balance, soil and snow hydrology, and plant physiology, as well as carbon-nitrogen cycling, mostly using process-based methods. Specifically, the hydrological processes represented in the model include interception, canopy through-fall, infiltration, evaporation, transpiration, surface runoff, subsurface drainage, vertical soil moisture flux through vadose zone soil, and groundwater discharge and recharge. The model also determines changes in vegetation states (carbon and nitrogen pools in various plant compartments) based on simulated ecosystem processes such as photosynthesis and respiration. CLM 4.5 requires hourly meteorological forcing data (air temperature, humidity, rainfall, and radiation), soil texture for its 10 computational layers down to a 3.8 m depth, and percent cover for the model's pre-set PFTs. The broadleaf evergreen shrub and broadleaf deciduous shrub PFT parameterizations in CLM were developed to represent shrubs in arid and semiarid regions in the world, including deserts in southwestern U.S. (Zeng et al. 2008). CLM4.5 requires inputs for meteorological values, including air temperature, precipitation, radiation, air pressure, and humidity, which we provided at an hourly frequency. An interpolation module within CLM 4.5 further downscaled the meteorological data for the model's half-hourly computational time-stepping (Oleson et al., 2010).

It should be noted that recently, some ecohydrological models have further incorporated plant hydraulics (water transport within the plant) (e.g., CLM5 (Lawrence et al., 2018)) and/or plant demography (evolution of plant age distribution) (see review by Fisher et al., (2018)), which are likely capable of providing a more accurate representation of the ecohydrological response to climate variability. However, such model approaches require many parameters that are highly uncertain, currently posing obstacles to their widespread use. In this study, prompted by the growing observations of leaf trait variability (Kattge et al., 2011), we chose to focus on leaf traits as well as other traits already included in common ecohydrological models, without introducing plant hydraulics or demographic modules. Our approach can be extended in the future to further consider parameters for models that include such modules.

#### 2.4. Model-data fusion approach for parameter estimation

We use the ensemble Kalman Filter (EnKF) method (Evensen, 1994) to estimate plant trait parameters in the CLM4.5 model based on observations. Although the method was originally developed for estimating model states (i.e., variables simulated by the model), we use the "augmented state" extension, with which model parameters can also be estimated (Evensen, 2009). EnKF has been commonly used in hydrological applications (Reichle et al., 2002; Moradkhani et al., 2005; Liu and Gupta, 2007; Reichle et al., 2008), and more recently also in ecological studies (Raupach et al., 2005; Williams et al., 2005; Wang et al., 2009; Luo et al., 2011). The basic idea of EnKF is that observations are used to constrain the model over a sequence of "assimilation cycles" that cover observational times. One assimilation cycle comprises two steps: a model "forecast" step, in which an ensemble of model runs are carried out to represent initial model information and its uncertainty, and a model "analysis" step, which uses the following equation to constrain (or "condition") the model using an observation at time  $t(y_t)$ :

$$X_t^a = X_t^f + K(y_t - HX_t^f),$$

where

$$K = P_t^f H^T (HP_t^f H^T + R)^{-1}$$

is known as the "Kalman gain."  $X_t^f$  and  $X_t^a$  are vectors of model state variables at time t that includes states and parameters, with the "f" superscript indicating the forecast state (before the observation constraint) and the "a" superscript indicating the analysis state (after the observation constraint). H is the function that determines the relationship between model states and observation data. To represent uncertainties,  $P_t^f$  is the forecast error covariance matrix and is determined from the ensemble of model runs, and R is the observation error covariance matrix. The forecast step in the assimilation cycle at time t+1 step uses the analysis vector  $X_t^a$  at previous time step (time t) as the initial state; the assimilation cycle evolves until the final time step of available observational data.

We used two different implementations of EnKF that were previously presented in Liu and Ng (2019). Both implementations included two computational passes of the EnKF for the whole observational period (from t = 0 to T) to help resolve inconsistencies that can arise between state and parameters estimates when using Kalman filter type methods with strongly nonlinear models. Experiments E1 and E2 utilized the "static" implementation of the two-pass EnKF from Liu and Ng (2019), which treats parameters as constant in time and consists of a relatively straightforward extension of the standard EnKF over two passes to constrain uncertainties. Experiment E3 used the "stochastic" implementation of the two-pass EnKF, which was developed by Liu and Ng (2019) to constrain temporally dynamic parameterizations of plant functional traits and to identify potential trait variability. The main way that the stochastic implementation of the EnKF differs from the standard static implementation is that instead of using only the final parameter estimate at the last time step of the calibration period, we focus on the time-varying parameter estimates over the entire time period, and this enables us to identify how trait parameters co-vary with environmental conditions. More implementation details can be found in Liu and Ng (2019). Liu and Ng (2019) showed that the new stochastic implementation can uncover temporal trait variability, and its implementation at the Kelmet site vielded parameter time series estimates that were correlated with soil water stress. A regression-based parameterization based on this correlation allowed probabilistic predictions of trait variability and therefore the impacts on ecohydrological processes at Kelmet.

Similar to Liu and Ng (2019), we assumed in this study that model uncertainty arises due to uncertainties in eight plant parameters (Table S1); here, we further considered uncertainties in the following soil hydraulic properties to account for the effect of different soil conditions between the two study sites: the moisture retention curve exponent B, saturated hydraulic conductivity  $K_{sat}$ , saturated matric potential  $\Psi_{sat}$  and saturated volumetric soil moisture content  $\theta_{sat}$ . In CLM4.5, these parameters are used for calculating the unsaturated hydraulic conductivity and moisture retention curve. In all experiments, including E3, soil hydraulic parameters were treated as static in time. The initial distribution of plant trait parameters, prior to any constraint on observations, was adopted from Liu and Ng (2019), where three of the plant trait parameters were derived from the global plant trait database TRY (Kattge et al., 2011) with lognormal distributions, and the other five plant parameters, which are generally not found in TRY, were assumed to follow the uniform distributions obtained from White et al. (2000) (Table S1). It should be noted that LAI is a prognostic state variable in CLM 4.5 instead of an input parameter/states in many other land-surface models. The initial distributions of soil hydraulic parameters, prior to any constraint on observations, were assigned based on the method from Ng et al. (2014). The MODIS LAI and soil moisture measurement at 15 cm and 35 cm depths were used for the observational constraints in the EnKF implementation.

#### 2.5. Downscaled future climate data under the RCP scenarios

We obtained the new statistically downscaled climate model dataset, Multivariate Adaptive Constructed Analogs version 2

meteorological data (MACAv2-METDATA), for our future model predictions. This data product contains daily downscaled meteorological variables for the conterminous U.S. at 4-km resolution under the RCP 4.5 and RCP 8.5 scenarios. GHG emissions peak around the year 2040, and then stabilize in RCP 4.5, while GHG emissions continue to rise throughout the 21st century in RCP 8.5. The meteorological variables in MACAv2-METDATA were statistically downscaled from global climate model (GCM) data from the Coupled Model Intercomparison Project 5 (CMIP5, Taylor et al. 2012). Here, we used MACAv2-METDATA derived from the Geophysical Fluid Dynamic Laboratory (GFDL)-ESM2M output (Delworth et al., 2006), including 2 m air temperature, precipitation, shortwave radiation, and vapor pressure deficit.

We then disaggregated the daily meteorological forcing data from MACAv2-METDATA into 1-hourly time steps using the open source toolbox MEteoroLOgical observation time series DISaggregation Tool (MELODIST) (Förster et al., 2016). We tested the disaggregation algorithms using observed meteorological time series (from 1961 to 2009) for the Kelmet and Globe sites and found that they produced a reasonable reconstruction of diurnal features at those sites (Fig. S1).

#### 3. Results and discussion

#### 3.1. Temporal and spatial variability in trait estimates

In all experiments, soil hydraulic parameters were assumed to be spatially variable at the two sites to account for the observed difference in soil properties with elevation (Bedford et al., 2009). Within a site, the soil parameter estimates using the two-pass EnKF were similar across all three experiments, which is unsurprising because the experiments differed only in their treatment of plant parameters. Results for E1 in Fig. 3 show that the higher elevation Globe site has greater values of B,  $\Psi_{sat}$ , and  $\theta_{sat}$ , but lower  $K_{sat}$ , compared to the lower elevation Kelmet site. These soil parameter estimates are consistent with having younger and coarser soils deposited at lower elevations in the Mojave Desert (Rundel and Gibson, 2005; Bedford et al., 2009; Miller et al., 2009).

Fig. 4 shows the plant trait estimates from the second (last) EnKF pass for the broadleaf-evergreen-shrub PFT in each of the three experiments at the two sites. Note that although only the final time parameter estimate is used as the result in the static EnKF implementations in E1 and E2, we show the entire observational period in order to facilitate comparisons with the E3 result, which uses the full time series of the temporally varying parameter estimate as the result. Although all trait parameters for the broadleaf-evergreen-shrub PFT were relatively well-constrained in the first pass of EnKF (the ranges of parameter estimates were all reduced compared with their prior distributions, see Fig. S2), SLA and rootb (representing rooting depth) parameters for the broadleaf-evergreen-shrub PFT had the greatest uncertainty reduction in all experiments. When spatial variability was allowed in traits in E2 and E3, we found a higher SLA and lower rootb estimate at the Globe site compared to at the Kelmet site. In addition, in E3, estimated SLA for the broadleaf-evergreen-shrub PFT at both sites showed clear temporal dynamics using the stochastic implementation (coefficient of variation of 0.25 and 0.19 for Kelmet and Globe site, respectively), providing model evidence for SLA variability over time in the broadleaf-evergreen-shrub PFT; none of the other plant parameters showed appreciable temporal variability (coefficient of variation < 0.1), including SLA for the broadleaf-deciduous-shrub PFT.

Although direct trait observations were not available at our study sites to validate the results of our model-data fusion approach, our variable SLA and root depth estimates are consistent with data from other studies. Spatial variations in plant functional traits have been widely observed across global biomes, and plant functional type and climate gradient are identified as the main drivers for the trait divergence (Wright et al. 2005; Kattge et al., 2011; Osnas et al., 2018). In particular, SLA variability has been found to be an indicator of plant adaptation to climate variability, and the plant with high plasticity in

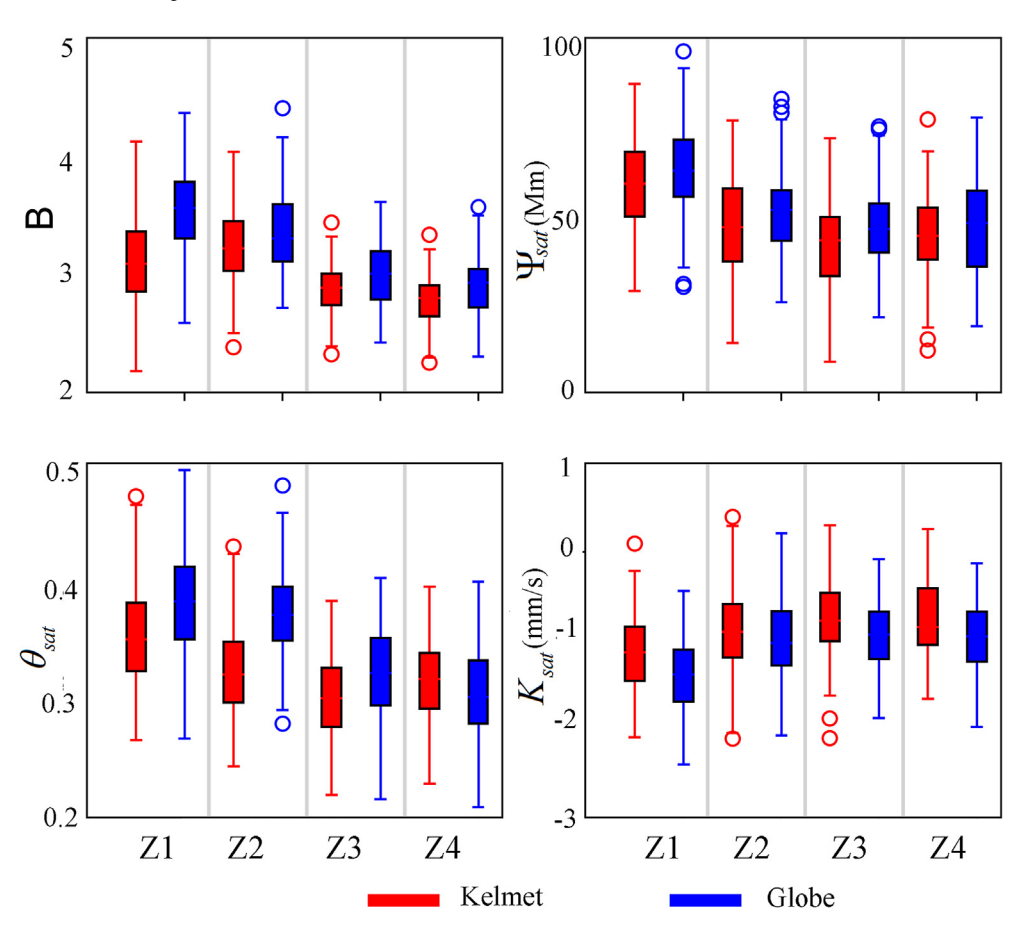


**Fig. 3.** Boxplots showing the distributions for estimated soil hydraulic parameters for the Kelmet (red) and Globe (blue) sites over the depth intervals of Z1: 0–1.8 cm, Z2: 1.8–4.5 cm, Z3: 4.5–9.1 cm, and Z4: 9.1–380 cm. Boxes represent the interquartile range (from 25th to 75th percentile), whiskers represent the extreme values (within 1.5 times the inter-quartile range from the upper or lower quartile), and circles represent outliers.

SLA tend to have high resource-use efficiency under varying environment conditions (Niinemets, 2001; Poorter et al., 2009). Consistent with our estimate of smaller SLA at the hotter and drier Kelmet site, decreases in SLA with lower water availability have been observed across space in evergreen species (Wright et al., 2001; Schulze et al., 2006; Gouveia and Freitas, 2009), grasses (Oyarzabal et al., 2008; Meng et al., 2015), and crops (Pandey et al., 1984; Craufurd et al., 1999). Dry climate favors small, thick, and dense leaves (low SLA), and this adaptation allows plant to increase water use efficiency (Niinemets,

1999). As for rooting depth, regional climate, topography, and local soil properties can be potential drivers for its variations (Stone and Kalisz, 1991; Fan et al., 2017). Again consistent with our estimate of greater rooting depth (larger rootb) at the Kelmet site, deeper roots are generally found in coarser and younger soils, which are characterized by vertically homogeneous soil texture and low field capacity (Sperry and Hacke, 2002; Schenk and Jackson, 2005). Hamerlynck et al (2002) found that *Larrea tridentata*, the main vegetation species at the Kelmet site, can utilize both deep and shallow roots to maintain continuous

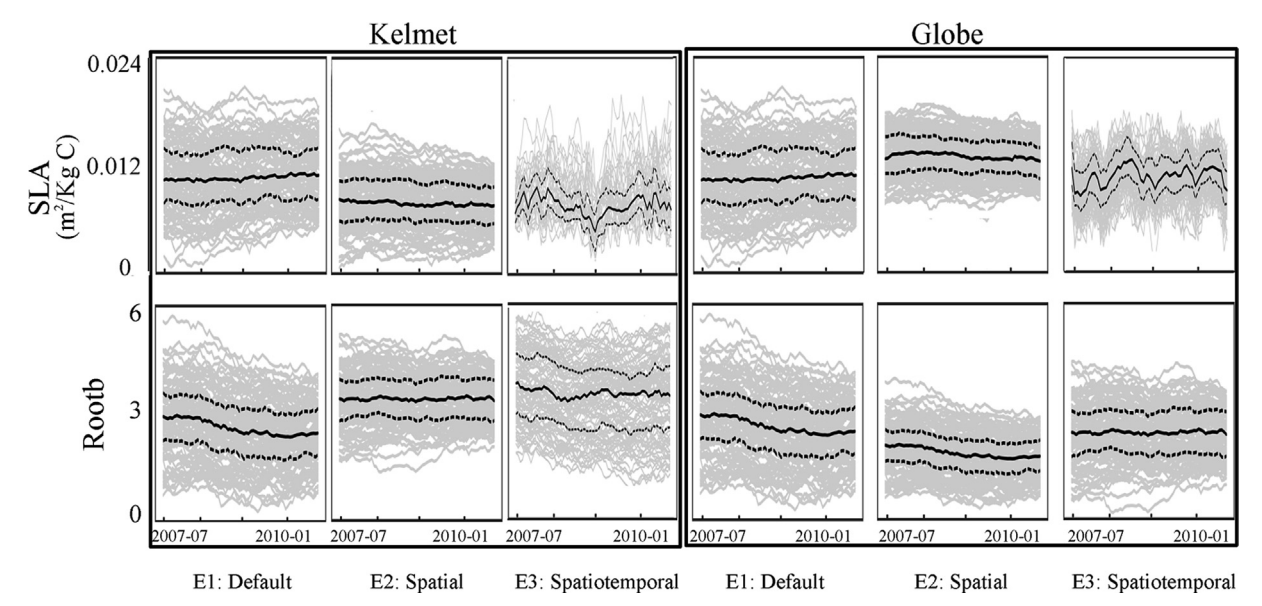


Fig. 4. Plant parameters (SLA and Rootb) estimation at the Kelmet site using the three parameterization methods (E1, E2, and E3).

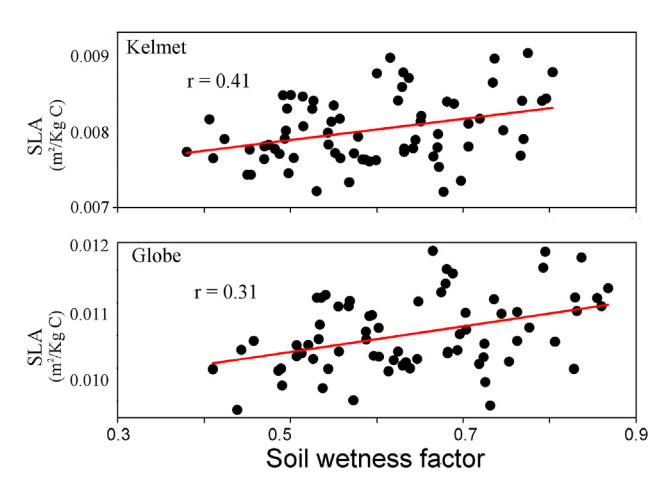


Fig. 5. Statistical relationship between estimated SLA and 30-day averaged soil wetness factor at the Kelmet and Globe sites.

photosynthetic activity, presumably by extracting shallow water during wet seasons and deeper water stores during droughts.

Less is known about temporal trait variability compared to spatial variability, likely because of challenges in repeat measurements. This gap prompted previous work by Liu and Ng (2019), which found SLA parameter estimates for the broadleaf-evergreen-shrub PFT exhibited temporal pattern and the variation was significantly correlated with available soil water at the Kelmet site. Here, our results show that the temporal variation of SLA estimates associated with water availability (in terms of soil wetness factor,  $\beta$ ) also occurs at the high elevation Globe site (Fig. 5), indicating that the potential for water-stress driven SLA spatiotemporal variability in the broadleaf-evergreen-shrub PFT could be widespread across the watershed. Though less studied than spatial variability, both biotic (e.g. leaf aging, Reich et al., 1991; Laclau et al., 2009) and abiotic factors (e.g. radiation, Serbin et al., 2014) have been found to be correlated with temporal SLA variability across a range of biomes (Dawson and Bliss 1993; Abrams 1994; Reich et al., 1997; Damesin et al., 1998; Wilson et al., 2000; Damesin and Lelarge, 2003; Xu and Baldocchi, 2003; Liu and Stützel, 2004; Grassi et al., 2005; Misson et al., 2006; Ma et al., 2011; Nouvellon et al., 2010; Dwyer et al., 2014). During drought seasons, plants commonly decrease SLA by modifying their anatomical tissues for less water requirement (Poorter et al., 2009). In addition to changes in leaf-scale SLA, water availability may also alter the plot (meters) and ecosystem (10's of meters)-scale SLA. In water-limited environments, drought events can trigger the selective fall of older high-SLA leaves or the dormancy of high-SLA species, resulting in lower average SLA values. For evergreen species that experience seasonal drought, previous studies (Misson 2006; Gratani and Varone, 2006; Nouvellon et al., 2010) found that SLA can be about 20%-28% lower during drought periods, which is consistent with our finding that soil water availability can be the driver for SLA temporal variation at the water-limited study sites. In addition to changes within individual plants, these seasonal shifts in SLA may also reflect changes in community-level distributions, as different species have been noted to exhibit unique relationships between SLA and water use strategy (Castro-Díez et al., 2000; Hassiotou et al. 2010; Ma et al., 2011; De la Riva et al. 2016; Peguero-Pina et al. 2017).

## 3.2. Comparison of variability in estimated SLA between sites

## 3.2.1. Temporal variability in estimated SLA

To examine how the temporal variability in estimated SLA compares across sites, we followed the approach of Liu and Ng (2019) and built linear regression relationships for each of the two sites based on the estimated parameters from E3 with two explanatory variables: SLA(t-30), SLA at the previous 30-day time step and  $\bar{\beta}$ , the soil

wetness factor averaged over the preceding 30 days. Fig. S3 shows that both regression models can well match the SLA estimation for the Kelmet and Globe sites, respectively. Note that the regression coefficients of the two equations are different (see the caption of Fig. S3 for the statistical significance in their differences), with higher sensitivity of SLA to soil water availability and a lower auto-correlation coefficient value at the Kelmet site. Assuming that this difference in the estimated SLA sensitivity between sites captures actual conditions, it may reflect the different species compositions at the two sites. Varying sensitivity of SLA in response to water stress within one PFT has been reported in previous experimental studies (Anyia and Herzog, 2004; Ramírez et al., 2012: Yin et al., 2004: Nielsen et al., 2019). For example, Liu and Stützel (2004) found that water stress decreased the SLA in four varieties of vegetable amaranth but with different sensitivity. In a semi-arid Mediterranean ecosystem, Ramírez et al (2012) conducted a manipulative drought field experiment with broadleaf evergreen shrubs and reported greater SLA response to water availability in species with higher SLA. In contrast to Ramírez et al (2012), however, we found higher SLA sensitivity in Kelso Valley to occur at the site with lower estimated SLA for the broadleaf-evergreen-shrub PFT (Kelmet) rather than higher SLA (Globe). It is possible that only two years of indirect coarse-resolution LAI and spatially sparse soil moisture data in our study may be inadequate for fully constraining the actual SLA sensitivity to soil water availability. Another possibility that has not been previously explored is that climatic differences between sites may trigger varying levels of trait sensitivity to environmental stressors, in addition to species type. Further research into trait variability across species and climates is needed. Overall, our results suggest that moisture-driven temporal trait variability may occur widely across desert shrublands, but that their implementation in models could remain a challenge due to unique location and/or species-specific relationships.

#### 3.2.2. Spatial versus temporal variability in estimated SLA

The little attention paid to temporal trait variability relative to spatial prompted us to next evaluate how the two types of variability compare in our results for the E3 experiment. We found that the spatial differences in estimated SLA across the two sites were greater than the temporal range from 1961 to 2010 at both sites (Table 1). The positive relationship between temporally variable SLA estimates and simulated soil wetness found above (Fig. 5) suggests that wetter and cooler conditions at Globe compared to Kelmet could be driving the similarly positive spatial gradient in estimated SLA variability based on water availability at the two sites. The apparent SLA sensitivity to water availability (calculated by the change in SLA per change in soil wetness factor in the model) is in fact much greater over space than over time at each site; the spatial difference in soil wetness is even smaller than the temporal difference, even though the spatial difference in SLA is greater than the temporal difference. This indicates that estimated SLA changes more in between the study sites than would be expected due to the

Table 1 Comparison of the apparent SLA sensitivity to water availability (in terms of the soil wetness factor  $\beta$ ), over space (between Kelmet and Globe) and over time (from 1961 to 2010), for simulations from the spatiotemporal test E3. For calculating spatial calculation, we used the difference in long-term average SLA and soil wetness factor between the two sites, and for the temporal calculation, we used the minimum to maximum range in 30-day average SLA and soil wetness factor over the 50-year simulation period at each site.

	Spatial	Temporal		
		Kelmet	Globe	
$\Delta SLA(m^2/kg C)$ $\Delta \beta$	0.00337 0.08	0.00221 0.51	0.00289 0.48	
$\Delta SLA/\Delta \beta$	0.0421	0.0043	0.0060	

water stress driven temporal variability inferred at each site over the 40-year modeling period.

The greater spatial compared to temporal gradients found in our SLA estimates suggests that actual spatial trait variability may be more prominent than temporal, and this may be attributed to a couple of reasons. First, as suggested for the difference in temporal SLA characteristics at the two sites, distinct species compositions between the sites could exhibit divergent SLA characteristics (Niinemets, 2001; Poorter et al., 2009). Second, it is possible that persistent differences in climate and soil wetness conditions between the two sites have led to a greater change in SLA over space than is physiologically possible over the shorter, seasonal times scales of climatic changes within a site. An implication of our findings is that although traits can vary both spatially and temporally, easier-to-measure spatial variability characteristics should not be directly substituted into models to represent temporal variability. Verheijen et al (2015) recently developed regression models to build statistical relationships between plant trait parameters and climatic conditions using a global trait database and then used these to predict the anually dynamic trait parameters.

## 3.3. Ecohydrological role of spatial and temporal trait parameter variability

Comparing simulation results using parameter estimates from E1, E2, and E3 provides insights into the relative importance of spatial versus temporal variability in parameters for simulating ecohydrological states. The parameter estimates from the E1 experiment performed worse than those from E2 and E3 in reproducing the observed LAI and soil moisture at both the Globe and Kelmet sites (Figs. 6 and 7, respectively). When allowing for spatial variability of trait parameters in the E2 parameterization, simulated soil moisture improved at both sites, and simulated LAI matched the time-averaged LAI observations. However, the simulated LAI using trait parameter estimates from E2 failed to capture the seasonal LAI variations at both sites. When the temporally dynamic SLA estimates from E3 were incorporated in the model, simulations tracked LAI observation dynamics much more closely than the simulation that only accounted for spatial

variations in parameters (E2) (Fig. 6).

Simulations could be expected to show a more substantial change with the addition of spatially variable SLA compared to temporally variable SLA, given the greater spatial difference in estimated SLA than temporal (Table 1). Indeed, Table 2 quantitatively shows that the greatest improvement (increase in the coefficient-of-correlation (R<sup>2</sup>) and decrease in root-mean-square-error (RMSE)) in LAI and soil moisture simulations occurred when spatial variability of trait parameters was allowed in CLM 4.5 (E1 to E2). Note that E1 already took into account differences in soil and climate conditions between the sites, and so E2 results point to the need for including spatial variability in plant trait parameters to capture both ecological and hydrological states. Further incorporation of temporally variable trait parameters in E3 led to a subtler improvement in model performance (Table 2), suggesting that ecohydrological process simulations were more sensitive to the spatial variability of trait parameters. However, compared to the results in E3, most of the LAI ensemble uncertainties with temporally constant traits in E1 and E2 failed to include the LAI observations during the observation period at both sites (Fig. 6). This corroborates findings at the lower elevation Kelmet site by Liu and Ng (2019) and demonstrates the benefit of using temporally variable SLA for robustly capturing LAI seasonal variation across a soil and climate gradient, such that model ensemble predictions encompass actual conditions.

Overall, the simulations using the three sets of parameter estimates demonstrate that both spatial and temporal variability in the SLA and rooting depth parameters impact LAI and soil moisture simulations over the observation period. This is consistent with the ecological functions of the traits represented by these parameters: SLA is a key ecophysiological trait affecting photosynthetic capacity and plant biomass (Reich et al., 1997; Niinemets, 1999; Antúnez et al., 2001; Wright et al., 2004; Quero et al., 2006), and rooting depth is a trait that is central to determining ecosystem resilience to water stress and long-term coupling between carbon and water cycles (Nepstad et al., 1994; Oliveira et al., 2005; Maeght et al., 2013).

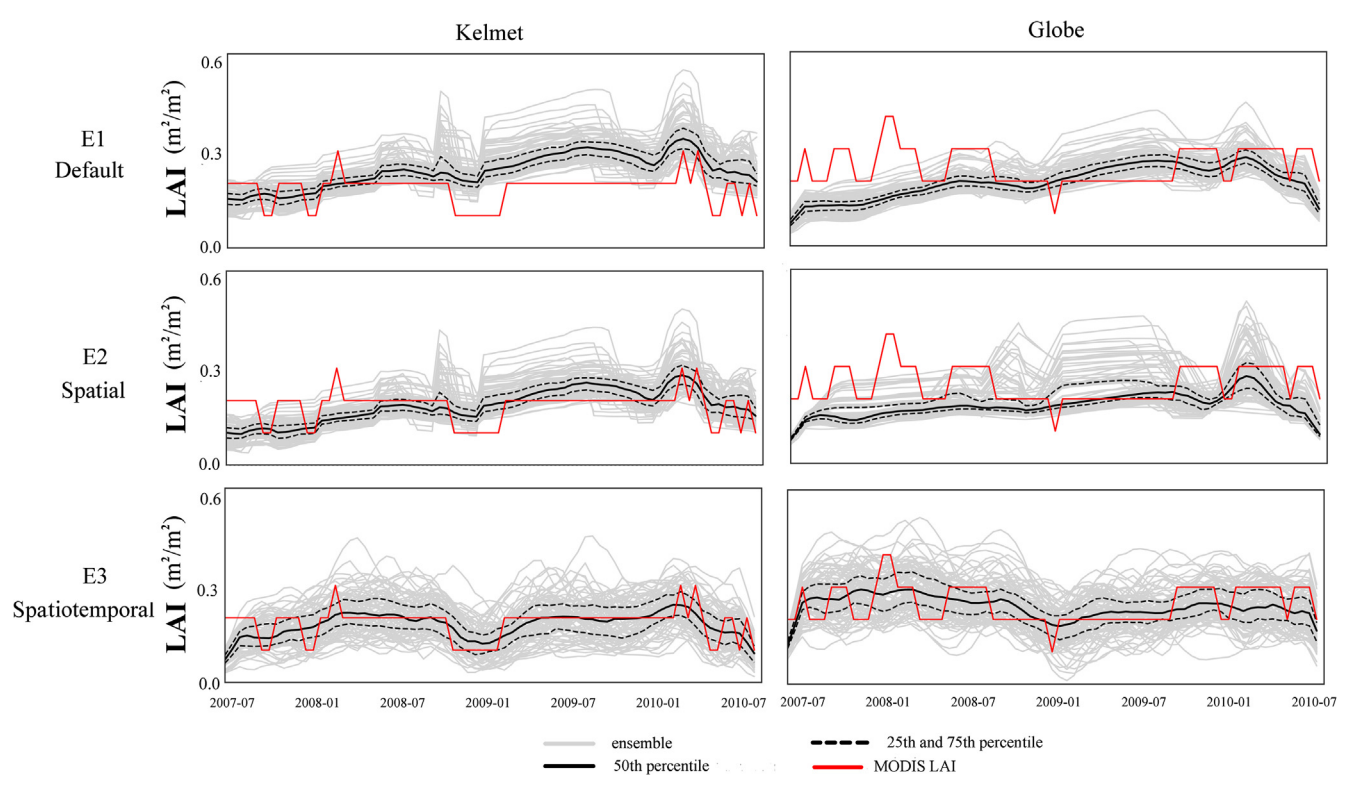


Fig. 6. Comparison of calibrated simulated LAI and MODIS LAI in the three parameterization schemes (E1, E2, and E3).

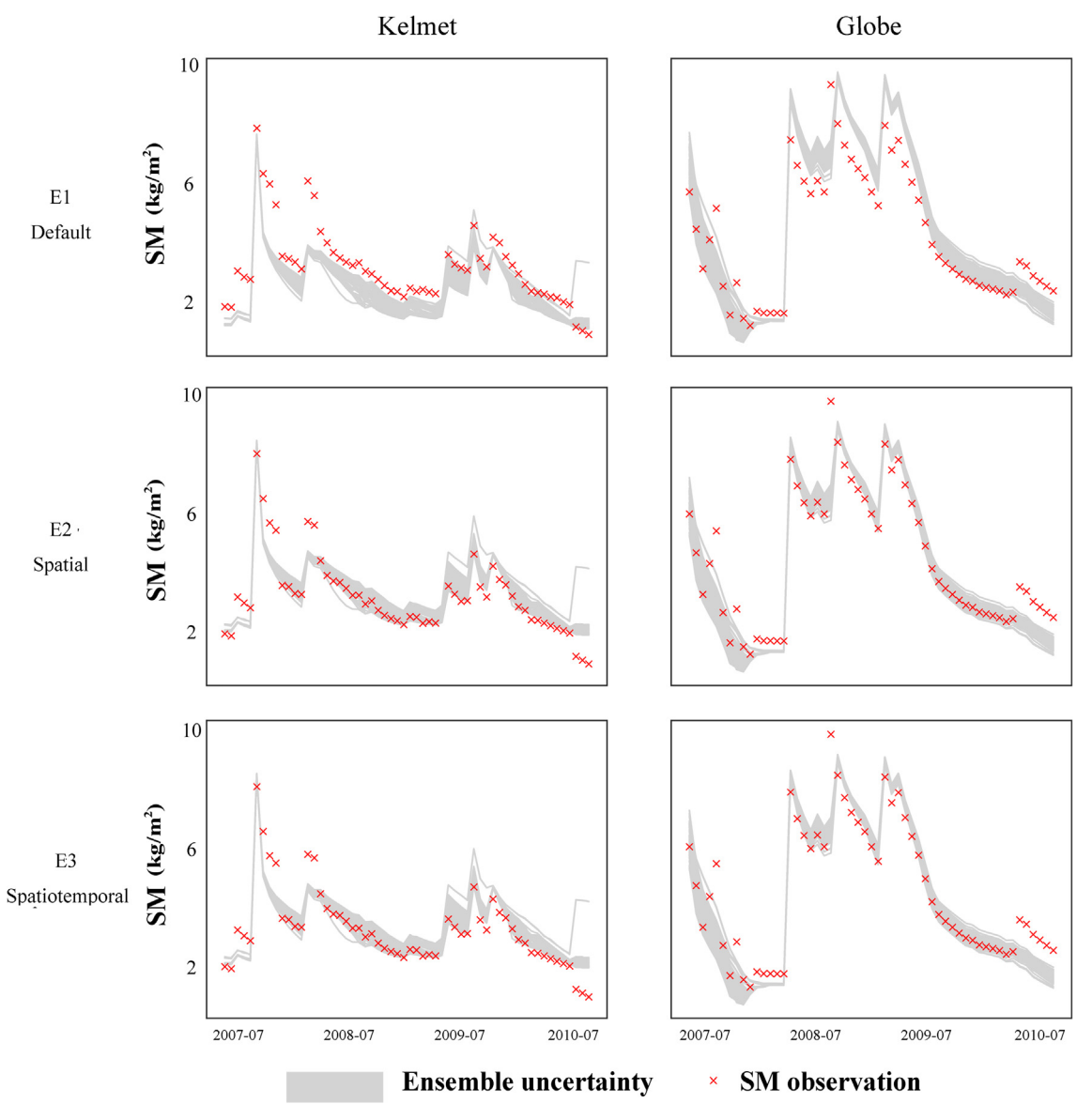


Fig. 7. Comparison between calibrated simulated soil moisture (SM) (kg/m²) (grey line) and in-situ observations (red) in the E1, E2 and E3 parameterization schemes

Table 2 Model coefficient-of-correlation with observations ( $R^2$ ) and model root mean square error (RMSE) for leaf area index (LAI) and soil moisture (SM) among the three calibrated simulations (E1, E2, and E3) at the Kelmet and Globe sites.

		Kelmet			Globe		
		E1	E2	E3	E1	E2	E3
LAI (m <sup>2</sup> /m <sup>2</sup> )	R <sup>2</sup> RMSE R <sup>2</sup>	0.18 0.12	0.19	0.29	0.12 0.23	0.14 0.16	0.17 0.11
SM (kg/m <sup>3</sup> )	RMSE	0.58 3.76	0.62 1.04	0.61 1.05	0.51 4.71	0.57 1.45	0.57 1.43

#### 3.4. Future scenario simulations with trait parameter variability

Using a 40-year historical period at the Kelmet site, Liu and Ng (2019) showed that simulations with temporally variable SLA in the broadleaf evergreen shrub PFT had greater simulated water use efficiency compared to the case of time-static SLA. Here, we further evaluated how the combination of spatial and temporal trait parameter variability impacts simulated ecohydrological fluxes, and we further

assessed how that variability might affect predictions of coupled carbon and water fluxes under future climate change. To do this, we extended experiments E1, E2, and E3 by implementing their respective parameter estimates in simulations forced with RCP climate scenarios from 2011 to 2100 for the two sites. We first focused on the most pessimistic climate scenario, RCP 8.5, in order to bracket our predictions of ecohydrological changes with the various trait parameter inputs. For E1 and E2, the estimated parameters at the final time step were used to run CLM 4.5; for E3, the regression equations for time-varying SLA for the two sites (Fig. S3) were incorporated into CLM 4.5.

Fig. 8a, 8b, 9a, and 9b show the projections of climate forcing under the RCP 8.5 scenario at Kelmet and Globe. At both sites, temperature was predicted to rise and precipitation to decrease from 2011 to the end of 21st century with RCP 8.5. As a result, LAI was predicted to decrease at both sites for all experiments (Fig. 10 and Table S2). Specifically, across all experiments, LAI was estimated to decrease about 50% at Kelmet and 30% at Globe, with the more dramatic drop at Kelmet resulting from the more severe (warmer and drier) climatic conditions projected at that low elevation site. It should be noted that the LAI predictions in 2011 are higher than in the calibrated simulation period

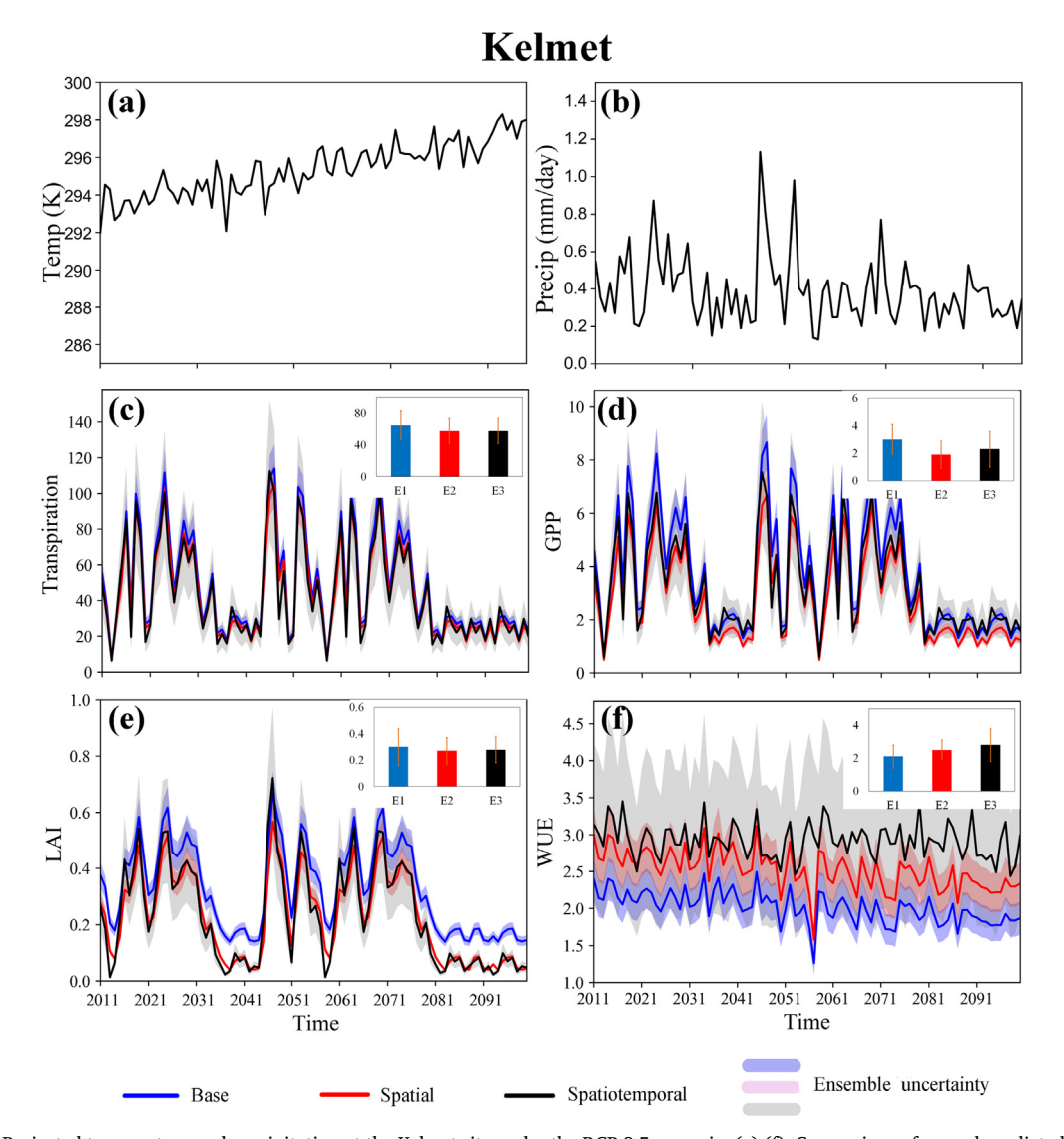


Fig. 8. (a) and (b): Projected temperature and precipitation at the Kelmet site under the RCP 8.5 scenario; (c)-(f): Comparison of annual predicted LAI, transpiration, GPP and WUE among the base (blue, E1), spatial (red, E2) and spatiotemporal (black, E3) simulations at Kelmet under the RCP 8.5 scenario. The small inset figures summarize the long-term average (2011–2099) annual variables based on the three simulations. The error bars show the ensemble standard deviation for the long-term (2011–2099) mean.

(from 2007 to 2010) at both sites, due to biases in the disaggregation scheme and possibly also in the climate model. In particular, Fig. S1 shows an over-representation of small rain events by the disaggregation scheme. Further, over-simulation of drizzle is a well-recognized problem in numerical weather prediction and climate models (Wood, 2005; Sun et al., 2006; Wyant et al., 2007; Hannay et al., 2009; Stephens et al., 2010). While this raises uncertainties in the absolute raw CLM outputs generated with climate model forcings, the simulations are nonetheless useful for examining relative trends over the century and relative differences among the three different experiments.

Demonstrating the sensitivity of future predicted ecohydrological fluxes to trait parameter variability at Kelmet and Globe, Figs. 8 and 9 respectively compare the simulated annual LAI, transpiration, gross primary productivity (GPP), and water use efficiency (WUE, defined as GPP divided by transpiration) under the RCP 8.5 scenario for the three experiments. Although the RCP 8.5 ensemble time series for the three experiments show overlaps, accounting for spatial differences in the broadleaf-evergreen-shrub trait parameters (E2 and E3 compared to E1) resulted in consistently lower estimated mean SLA at Kelmet (Fig. 4), and correspondingly lower simulated LAI, transpiration, and GPP (Fig. 8 and Table S3), while it led to the opposite effect at the Globe site

(generally higher SLA, LAI, transpiration, and GPP predictions) (Figs. 4 and 9 and Table S3). Unsurprisingly, including spatially variable trait parameters led to greater predicted differences in ecohydrological variables between the two sites, compared to the default parameterization (E1) (Table S3). Figs. 8 and 9 further demonstrate that the ensemble simulations using the temporally variable SLA estimates (E3 experiment) not only generated higher LAI seasonal variability due to time-varying SLA (especially at Kelmet, Fig. S4), but interestingly, they also show slightly higher long-term average LAI results than the simulations with only spatially variable SLA estimates (E2) (4 to 7% higher). The slightly higher LAI prediction with temporally dynamic SLA in E3 (compared to E2) corresponds to greater long-term average predicted GPP and WUE at both sites (insets in Figs. 8 and 9 and Table S3). Overall, our model results suggest that spatial variability in plant trait parameters can affect predictions of ecological and hydrological function (appreciable changes in GPP and transpiration), while temporal variability impacts may be more limited to the prediction of ecological responses (appreciable changes in GPP but not in transpiration, see insets in Figs. 8 and 9 and Table S3).

Our model-based evidence for trait variations affecting predicted ecohydrological processes across Kelso Valley is consistent with

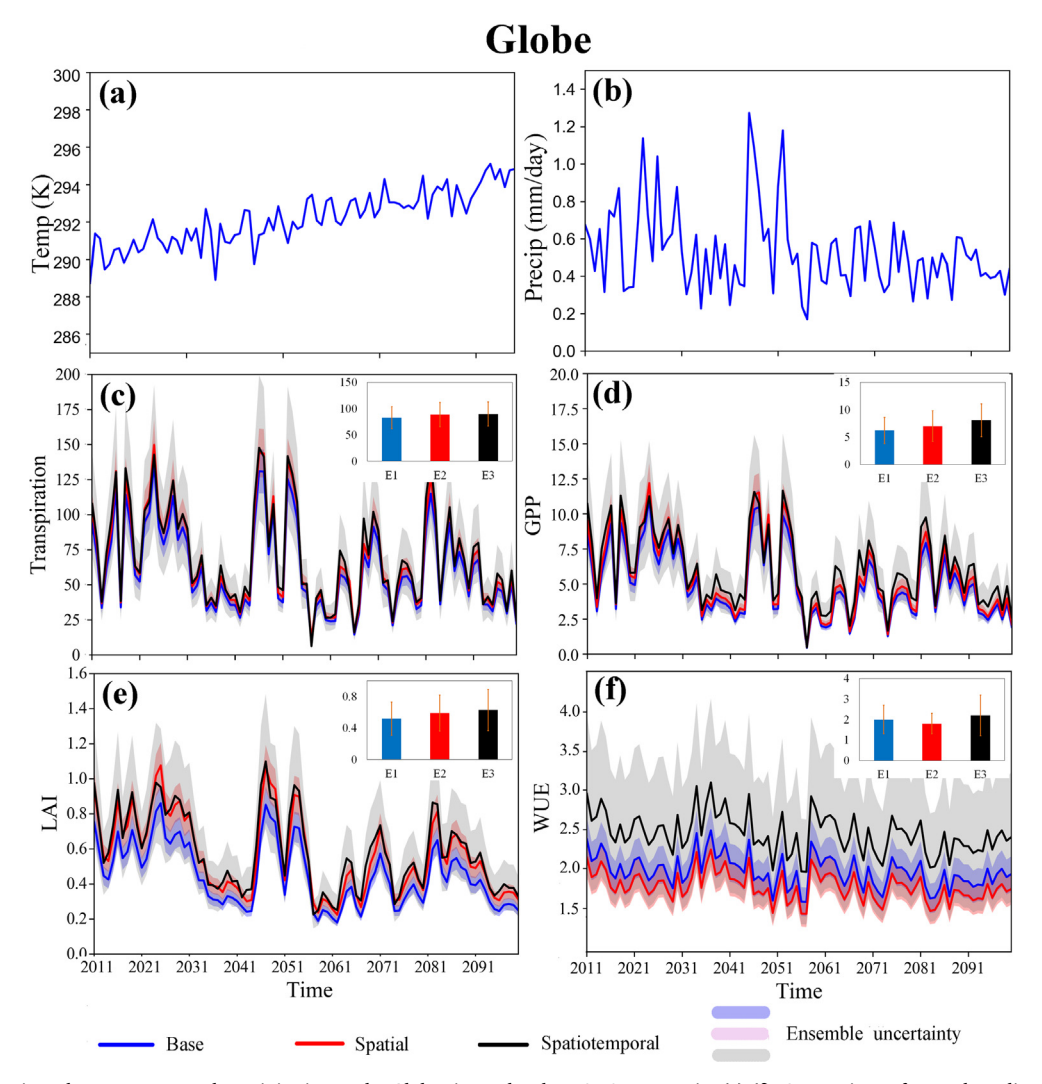


Fig. 9. (a) and (b): Projected temperature and precipitation at the Globe site under the RCP 8.5 scenario; (c)-(f): Comparison of annual predicted LAI, transpiration, GPP and WUE among the base (blue, E1), spatial (red, E2) and spatiotemporal (black, E3) simulations at Globe under the RCP 8.5 scenario. The small inset figures summarize the long-term average (2011–2099) annual variables based on the three simulations. The error bars show the ensemble standard deviation for the long-term (2011–2099) mean.

observations from other studies. Gouveia and Freitas (2009) assessed intra-specific variation in a range of leaf attributes and leaf carbon isotope concentration in an evergreen tree Quercuset suber along a rainfall gradient and demonstrated that the changes in leaf thickness associated with water availability strongly affected the water use efficiency. Maxwell et al. (2018) measured the intrinsic water use efficiency (iWUE) (defined as the ratio of net carbon assimilation to stomatal conductance) along a 1500 m elevation gradient with a wide climatic range in a montane forest system and found that iWUE highly depends on the dominant evergreen forest species, leaf trait characteristics, and stage of soil development. Although these observational studies reported only spatial gradients in leaf traits, iWUE may also reflect temporal changes, because iWUE is derived from leaf carbon isotope values, which record accumulated plant conditions over time (Wieser et al., 2018). It should be noted that different species may have distinct strategies in response to environmental stressors, resulting in varying effects on ecohydrological processes. For example, some species with lower SLA have thicker leaves that support greater photosynthesis per area (De la Riva et al. 2016; Peguero-Pina et al. 2017), while other species with lower SLA have increased leaf density and reduced mesophyll conductance and photosynthesis (Castro-Díez et al., 2000; Hassiotou et al. 2010; De la Riva et al. 2016). Therefore, although evergreen species tend to show higher WUE with lower SLA, this relationship may not extend across different ecosystems. In terms of nutrients, trait variations have been shown to influence nitrogen cycling at the watershed scale due to differences within one PFT in litter quality (e.g. the ratio of carbon to nitrogen) and nitrogen uptake rates (Williard et al., 2005; Dawson et al., 2005). These previous studies suggest that simulated ecohydrological responses to trait parameter changes in our model may reflect actual sensitivities. Further research is needed to corroborate findings with field data and to evaluate the generality of the spatiotemporal trends found for Kelso Valley.

#### 3.5. Sensitivity to future climate scenario

To assess the impact of trait parameter variability on model predictions under a range of climate scenarios, we conducted additional simulations using the RCP 4.5 climate projections and compared results against those using the RCP 8.5 climate inputs. In RCP 4.5, temperature peaked around 2040 and then stabilized, following GHG emissions (Figs. S5a and S6a). Although both RCP scenarios showed that precipitation decreases at the end of 21st century, the decrease in RCP 4.5 was generally less severe (Figs. S5b and S6b). Qualitatively, compared to the case with only spatial trait variability, including spatiotemporal SLA variability had similar effects on the predicted ecohydrological variables as in the RCP 8.5 results – higher predicted time-averaged

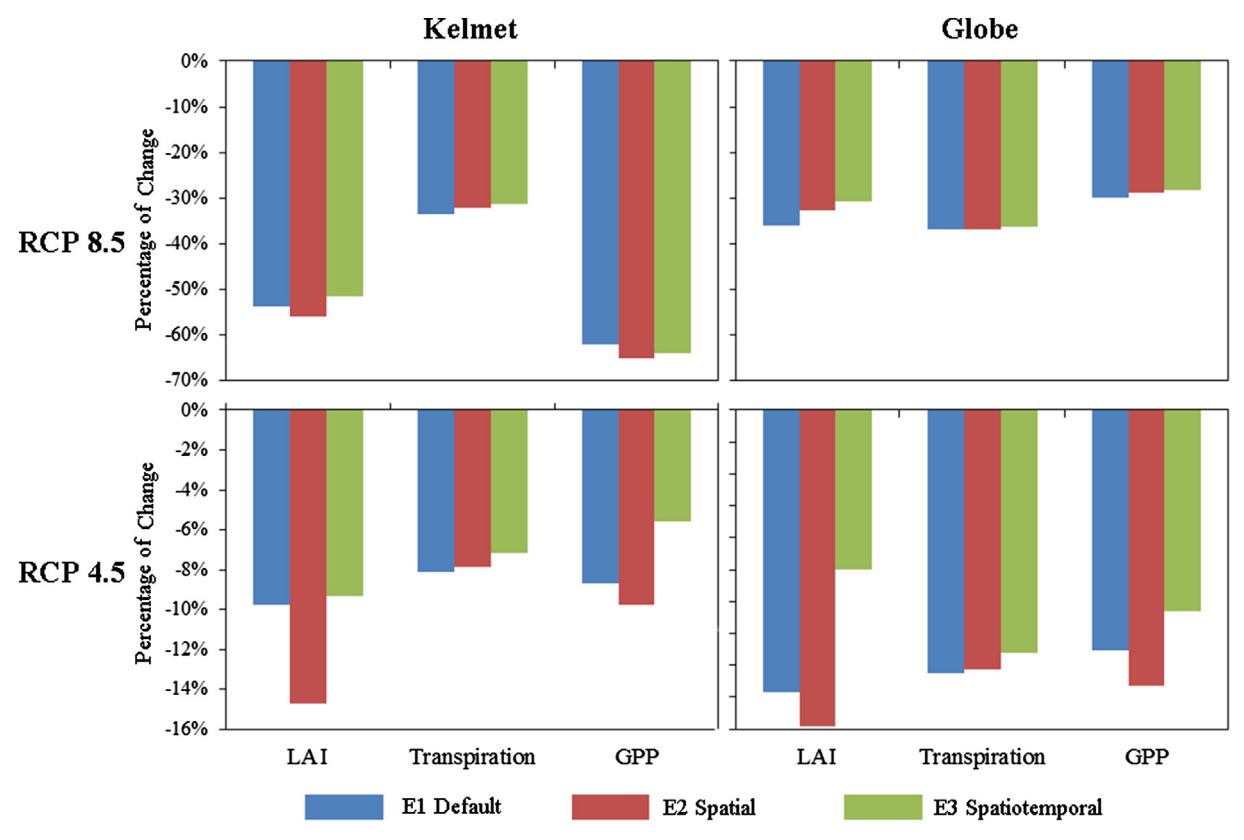


Fig. 10. Comparison of percent change in time-averaged, predicted LAI, transpiration and GPP between the two RCP scenarios at the Kelmet and Globe site. The percent change in LAI is calculated as (Average<sub>2090-2100</sub> – LAI<sub>2010-2000</sub>)/ LAI<sub>2000-2010</sub> × 100%.

LAI, GPP, and WUE, but approximately the same transpiration (Figs. S5 and S6 and Table S4).

Importantly, although both climate scenarios show that predicted WUE improves with temporally variable trait parameters (compared to the case with only spatial variability) (Tables S3 and S4), under the RCP 8.5 climate change projection, this has a far less effect on predicted LAI decline over 90 years (see similar percent change in LAI for all RCP 8.5 experiments in Fig. 10 and Table S2). The reason is that under RCP 8.5, the higher WUE simulations with temporally variable SLA (in E3 compared to E2) corresponded to only a small boost to the change in GPP over the 90-year period (boost of 0.2 gC/month at Kelmet and Globe, respectively, Table S2) compared to the initial GPP values (about 5.1 and 7.5 gC/month at Kelmet and Globe, respectively, Table S2), due to continuously warming and drying conditions. In fact, the 90-year relative declines in average LAI, GPP, and transpiration predictions under RCP 8.5 are very similar across all three experiments (Fig. 10 and Table S2), indicating that the magnitude of ecohydrological change simulated over the century with the most pessimistic climate scenario will overwhelm any potential benefits (higher WUE) that may be afforded by spatiotemporally variable trait parameters. In contrast, with the milder RCP 4.5 climate change projections, the improved WUE predictions with temporally variable SLA (E3, compared to only spatially variable traits in E2) correspond to a larger effect on predictions of relative LAI and GPP change over 90 years (Fig. 10). For example, at the Kelmet site, in the RCP 4.5 scenario, the higher WUE predictions with temporally variable SLA can appreciably buffer the simulated GPP (and LAI) decline from a 9.8% (and 14.7%) decline with only spatially variable SLA to a 5.6% (and 8.6%) decline with spatiotemporally variable SLA (Table S5 and Fig. 10). The simulation comparison between the two scenarios indicates that when considering spatiotemporally variable trait parameters, the benefits for ecohydrological processes depend on the long-term climate projections. Under the more pessimistic RCP 8.5 climate projections, our simulations suggest that

the trait variability represented by our trait parameter estimates may not be able to keep pace with the rates of warming and drying in our desert shrubland sites. It should be noted, however, that over smaller climatic variabilities, such as those that occur on the time scale of seasons up to a few years, improved WUE with spatiotemporal trait parameters can result in notably higher GPP, even under RCP 8.5. For example, from the year 2073 to 2075 in the RCP 8.5 scenario, GPP at Globe jumps up from 1.5 to 6.0 gC/mon (factor of 4) with spatiotemporally variable trait parameters, compared to only from 1.5 to 4.7 gC/mon (factor of about 3) with constant traits.

## 4. Summary and conclusion

By using remotely sensed LAI and in-situ soil moisture measurements, we implemented a model-data fusion approach that constrained spatiotemporally variable parameters representing plant functional traits of shrubs in a Mojave Desert watershed. We found that the broadleaf evergreen shrub PFT at a lower elevation study site had lower SLA (26%) and deeper rooting depth (17%) estimates than at a higher elevation study site. In addition, we demonstrated that the SLA estimates co-varied over time with soil water availability at both sites, but with different levels of sensitivity to water stress. Spatial variability in the estimated SLA parameter was found to be 26% greater than the temporal variability in the watershed. Incorporating the spatially variable trait parameters into the CLM 4.5 ecohydrological model was more important than representing temporally variable parameters for correctly capturing time-averaged LAI and soil moisture observations and simulating ecohydrological fluxes/states; however, temporally variable SLA parameters were needed to simulate the observed seasonality in LAI.

Our model-based findings in a desert shrubland suggest that the global bias of spatial plant trait observations compared to temporal observations may be somewhat justified, if spatial trait variability

generally exceeds temporal, as found in our estimates. However, results at our two study sites suggest that temporally variable trait parameters could be widespread, and incorporating them into models may be needed for capturing seasonal responses to environmental stressors that could improve predicted ecohydrological efficiency (as represented by WUE). Unfortunately, our parameterization results showed that spatial and temporal trait variability exhibit distinct characteristics, and consequently, more commonly observed spatial trait variability should not be directly adopted to also represent under-observed temporal variability in traits.

Our estimates of variable SLA and root-depth are generally consistent with field-based studies of trait variability in other settings, including previous findings that spatial and/or temporal trait variability may represent adaptations that benefit ecological function. This indicates that our model-based results may provide insights into actual ecohydrological conditions in desert shrublands. Our modeling work prompts additional measurements of plant traits such as SLA and root-depth over both time and space across different shrub types. Such field data can be used to test hypotheses raised by our model results, such as whether differences in climate, terrain, and species in desert shrublands could be driving spatial trait variability, and whether SLA may exhibit sensitivities to water availability that are greater over space than time, possibly due to inter-species or climatic differences, or to time-lags in adaptations.

RCP future climate scenario tests showed that spatially variable trait parameters impacted predictions of both carbon and water fluxes, while additional temporal variability in SLA generated higher predictions in LAI, GPP, and WUE. Increased WUE predictions with added temporal trait variability resulted in discernible ecohydrological benefits under the milder climate scenario (RCP 4.5), but simulations under the most pessimistic greenhouse gas emissions scenario (RCP 8.5) showed that this increase in WUE predictions was insufficient for appreciably buffering against more extreme stresses. In particular, 90-year ecohydrological projections in the study watershed under RCP 8.5 showed 30–50% declines in LAI regardless of trait parameter variability.

Our plot-scale model findings about variable plant traits prompt further extensions of our method to regional and global simulations of coupled carbon and water dynamics. Our method can be implemented to constrain incomplete trait distributions from general plant databases such as TRY using global remote sensing data (e.g. LAI from MODIS as in the current study, and possibly soil moisture from SMAP (Entekhabi et al., 2010) in future work) along with any other available observations at different spatiotemporal resolutions. This approach has the potential to effectively and efficiently build statistical relationships between the data-constrained traits and biotic and abiotic factors in a targeted region or even at the global scale.

## **Author contributions**

SL, GCN designed and performed the research; SL and GCN wrote the paper.

## **Declaration of Competing Interest**

The authors declare that they have no known competing financial interests or personal relationships that could have appeared to influence the work reported in this paper.

#### Acknowledgements

This study was supported by funding from NSF (NSF-1724781). Minnesota Supercomputing Institute (MSI) at University of Minnesota-Twin Cities and the Cheyenne cluster at NCAR provided the supercomputing resources. We acknowledge the data from the TRY initiative on plant traits (http://www.try-db.org). The TRY initiative and

database is hosted, developed and maintained by J. Kattge and G. Bönisch (Max Planck Institute for Biogeochemistry, Jena, Germany). The dataset MACAv2-METDATA was produced with funding from the Regional Approaches to Climate Change (REACCH) project and the SouthEast Climate Science Center (SECSC). We acknowledge the World Climate Research Programme's Working Group on Coupled Modeling, which is responsible for CMIP, and we thank the climate modeling groups for producing and making available their model output. For CMIP, the U.S. Department of Energy's Program for Climate Model Diagnosis and Intercomparison provides coordinating support and led development of software infrastructure in partnership with the Global Organization for Earth System Science Portals. The authors thank Dr. James M. Andre (Granite Mountains Desert Research Center and UC Riverside Department of Biology) for helping to identify plant species at the Globe site in the Mojave Desert. The authors thank Dr. David R. Bedford (posthumously), Dr. David M. Miller, and Dr. Andrew Cyr (U.S. Geological Survey, Menlo Park, California, USA) for their work to collect and compile the meteorological forcing data and soil moisture measurements in Kelso Valley; Dr. David M. Miller also provided helpful comments on the manuscript. We acknowledge the National Parks Service (NPS) for access to the Kelso Valley study sites within the Mojave National Preserve. The data used in the study is provided in the supplement information. This work is dedicated to the memory of Dr. David R. Bedford, whose passion for understanding the geology and ecohydrology of the Mojave Desert provided the foundation of this study.

#### Appendix A. Supplementary data

Supplementary data to this article can be found online at https://doi.org/10.1016/j.jhydrol.2020.125088.

#### References

Abbott, M.B., Bathurst, J.C., Cunge, J.A., O'Connell, P.E., Rasmussen, J., 1986. An introduction to the European Hydrological System — Systeme Hydrologique Europeen, "SHE", 1: History and philosophy of a physically-based, distributed modelling system. J. Hydrol. 87, 45–59.

Abrams, M.D., 1994. Genotypic and phenotypic variation as stress adaptations in temperate tree species: a review of several case studies. Tree Physiol. 14, 833–842.

Ali, A.A., Xu, C., Rogers, A., et al., 2015. Global-scale environmental control of plant photosynthetic capacity. Ecol. Appl. 25, 2349–2365.

Alton, P.B., 2011. How useful are plant functional types in global simulations of the carbon, water, and energy cycles? J. Geophys. Res. Biogeosciences, 116.

Antúnez, I., Retamosa, E.C., Villar, R., 2001. Relative growth rate in phylogenetically related deciduous and evergreen woody species. Oecologia 128, 172–180.
 Anyia, A.O., Herzog, H., 2004. Water-use efficiency, leaf area and leaf gas exchange of

cowpeas under mid-season drought. Eur. J. Agron. 20, 327–339.
Band, L.E., Patterson, P., Nemani, R., Running, S.W., 1993. Forest ecosystem processes at

the watershed scale: incorporating hillslope hydrology. Agric. For. Meteorol. 63, 93–126.

Belanger, M.J., Miller, J.R., Boyer, M.G., 1995. Comparative Relationships between Some Red Edge Parameters and Seasonal Leaf Chlorophyll Concentrations. Can. J. Remote Sens. 21, 16–21.

Bedford, D.R., Miller, D.M., Schmidt, K.M., Phelps, G.A., 2009. Landscape-scale relationships between surficial geology, soil texture, topography, and creosote bush size and density in the Eastern Mojave Desert of California. In: Webb, R.H. (Ed.), The Mojave Desert: Ecosystem Processes and Sustainability. Univ. of Nevada Press, Reno, pp. 252–277.

Bonan, G.B., Levis, S., Kergoat, L., Oleson, K.W., 2002. Landscapes as patches of plant functional types: An integrating concept for climate and ecosystem models. Global Biogeochem. Cycles 16, 5–23.

Butler, E.E., Datta, A., Flores-Moreno, H., et al., 2017. Mapping local and global variability in plant trait distributions. PNAS 114, E10937–E10946.

Castro-Díez, P., Villar-Salvador, P., Pérez-Rontomé, C., Maestro-Martínez, M., Montserrat-Martí, G., 1997. Leaf morphology and leaf chemical composition in three Quercus (Fagaceae) species along a rainfall gradient in NE Spain. Trees - Structure and Function 11, 127–134.

Castro-Díez, P., Puyravaud, J.P., Cornelissen, J.H.C., 2000. Leaf structure and anatomy as related to leaf mass per area variation in seedlings of a wide range of woody plant species and types. Oecologia 124, 476–486.

Chapin, F.S., Mooney, H.A., Chapin, M.C., et al., 2002. Principles of Terrestrial Ecosystem Ecology. Springer, New York, pp. 472.

Chen, L., Wang, L., Ma, Y., Liu, P., 2015. Overview of Ecohydrological Models and Systems at the Watershed Scale. IEEE Syst. J. 9, 1091–1099.

- Craufurd, P.Q., Wheeler, T.R., Ellis, R.H., Summerfield, R.J., Williams, J.H., 1999. Effect of Temperature and Water Deficit on Water-Use Efficiency, Carbon Isotope Discrimination, and Specific Leaf Area in Peanut. Crop Sci. 39, 136–142. https://doi. org/10.2135/cropsci1999.0011183X003900010022x.
- Damesin, C., Rambal, S., Joffre, R., 1998. Co-occurrence of trees with different leaf habit: A functional approach on Mediterranean oaks. Acta Oecologica 19, 195–204.
- Damesin, C., Lelarge, C., 2003. Carbon isotope composition of current-year shoots from Fagus sylvatica in relation to growth, respiration and use of reserves. Plant, Cell Environ. 26, 207–219.
- Dawson, T.E., Bliss, L.C., 1993. Plants as Mosaics: Leaf-, Ramet-, and Gender-Level Variation in the Physiology of the *Dwarf Willow, Salix arctica*. Funct. Ecol. 7, 203–304
- Dawson, T.E., Findlay, S.E., Lovett, G.M., Weathers, K.C., Templer, P.H., 2005. Influence of Tree Species on Forest Nitrogen Retention in the Catskill Mountains, New York, USA. Ecosystems 8, 1–16.
- De La Riva, E.G., Olmo, M., Poorter, H., Ubera, J.L., Villar, R., 2016. Leaf mass per area (LMA) and its relationship with leaf structure and anatomy in 34 mediterranean woody species along a water availability gradient. PLoS ONE 11, 1–18.
- Delworth, T.L., Broccoli, A.J., Rosati, A., et al., 2006. GFDL's CM2 Global Coupled Climate Models. Part I: Formulation and Simulation Characteristics. J. Clim. 19, 643–674.
- Dwyer, J.M., Hobbs, R.J., Mayfield, M.M., 2014. Specific leaf area responses to environmental gradients through space and time. Ecology 95, 399–410.
- Entekhabi, D., Njoku, E.G., O'Neill, P.E., et al., 2010. The Soil Moisture Active Passive (SMAP) Mission. Proc. IEEE 98, 704–716.
- Evensen, G., 1994. Sequential data assimilation with a nonlinear quasi-geostrophic model using Monte Carlo methods to forecast error statistics. J. Geophys. Res. Oceans 99, 10143–10162.
- Evensen, G., 2009. Data assimilation: the ensemble Kalman filter. Springer Science & Business Media.
- Fan, Y., Miguez-Macho, G., Jobbágy, E.G., Jackson, R.B., Otero-Casal, C., 2017.
  Hydrologic regulation of plant rooting depth. Proc. Natl. Acad. Sci. 114, 201712381.
- Fisher, R.A., Koven, C.D., Anderegg, W.R.L., et al., 2018. Vegetation demographics in Earth System Models: A review of progress and priorities. Glob. Change Biol. 24, 35–54.
- Förster, K., Hanzer, F., Winter, B., Marke, T., Strasser, U., 2016. An open-source MEteoroLOgical observation time series DISaggregation Tool (MELODIST v0.1.1). Geosci. Model Dev. 9, 2315–2333.
- Fullana-Pericàs, M., Conesa, M.À., Soler, S., Ribas-Carbó, M., Granell, A., Galmés, J., 2017. Variations of leaf morphology, photosynthetic traits and water-use efficiency in Western-Mediterranean tomato landraces. Photosynthetica 55, 121–133.
- Gotsch, S.G., Powers, J.S., Lerdau, M.T., 2010. Leaf traits and water relations of 12 evergreen species in Costa Rican wet and dry forests: Patterns of intra-specific variation across forests and seasons. Plant Ecol. 211, 133–146.
- Gouveia, A.C., Freitas, H., 2009. Modulation of leaf attributes and water use efficiency in *Quercus suber* along a rainfall gradient. Trees Struct. Funct. 23, 267–275.
- Grassi, G., Vicinelli, E., Ponti, F., Cantoni, L., Magnani, F., 2005. Seasonal and interannual variability of photosynthetic capacity in relation to leaf nitrogen in a deciduous forest plantation in northern Italy. Tree Physiol. 25, 349–360.
- Gratani, L., Varone, L., 2006. Long-time variations in leaf mass and area of Mediterranean evergreen broad-leaf and narrow-leaf maquis species. Photosynthetica 44, 161–168.
- Grayson, R.B., Western, A.W., Chiew, F.H.S., 1997. Preferred states in spatial soil moisture patterns: Local and nonlocal controls. Water Resources Res. 33, 2897–2908.
- Hamerlynck, E.P., McAuliffe, J.R., McDonald, E.V., Smith, S.D., 2002. Ecological response of two Mojave Desert shrubs to soil horizon development and soil water dynamics. Ecology 83, 768–779.
- Hannay, C., Williamson, D.L., Hack, J.J., et al., 2009. Evaluation of Forecasted Southeast Pacific Stratocumulus in the NCAR, GFDL, and ECMWF Models. J. Clim. 22, 2871–2889.
- Hassiotou, F., Renton, M., Ludwig, M., Evans, J.R., Veneklaas, E.J., 2010. Photosynthesis at an extreme end of the leaf trait spectrum: How does it relate to high leaf dry mass per area and associated structural parameters? J. Exp. Bot. 61, 3015–3028.
- Kattge, J., Díaz, S., Lavorel, S., et al., 2011. TRY-a global database of plant traits. Glob. Change Biol. 17, 2905–2935.
- Laclau, J.-P., Almeida, J.C.R., Gonçalves, J.L.M., et al., 2009. Influence of nitrogen and potassium fertilization on leaf lifespan and allocation of above-ground growth in *Eucalyptus* plantations. Tree Physiol. 29, 111–124.
- Liang, X., Lettenmaier, D.P., Wood, E.F., Burges, S.J., 1994. A simple hydrologically based model of land surface water and energy fluxes for general circulation models. Journal of Geophysical Research: Atmospheres 99, 14415–14428.
- Liu, F., Stützel, H., 2004. Biomass partitioning, specific leaf area, and water use efficiency of vegetable amaranth (*Amaranthus spp.*) in response to drought stress. Sci. Hortic. 102, 15–27.
- Liu, S., Ng, G.H.C., 2019. A data-conditioned stochastic parameterization of temporal plant trait variability in an ecohydrological model and the potential for plasticity. Agric. For. Meteorol. 274, 184–194.
- Water Resour. Res. 43 (7). https://doi.org/10.1029/2006WR005756.
- Luo, Y., Ogle, K., Tucker, C., et al., 2011. Ecological forecasting and data assimilation in a data-rich era. Ecol. Appl. 21, 1429–1442.
- Ma, S., Baldocchi, D.D., Mambelli, S., Dawson, T.E., 2011. Are temporal variations of leaf traits responsible for seasonal and inter-annual variability in ecosystem CO<sub>2</sub> exchange? Funct. Ecol. 25, 258–270.
- Maeght, J.-L., Rewald, B., Pierret, A., 2013. How to study deep roots—and why it matters. Front. Plant Sci. 4, 299.
- Marron, N., Delay, D., Petit, J.-M., Dreyer, E., Kahlem, G., Delmotte, F.M., Brignolas, F., 2002. Physiological traits of two Populus  $\times$  euramericana clones, *Luisa Avanzo* and

- Dorskamp, during a water stress and re-watering cycle. Tree Physiol. 22, 849–858.
  Maxwell, T.M., Silva, L.C.R., Horwath, W.R., 2018. Integrating effects of species composition and soil properties to predict shifts in montane forest carbon–water relations.
- Proc. Natl. Acad. Sci. 115, 201718864. Mclean, E.H., Prober, S.M., Stock, W.D., Steane, D.A., Potts, B.M., Vaillancourt, R.E.,
- Byrne, M., 2014. Plasticity of functional traits varies clonally along a rainfall gradient in Eucalyptus tricarpa. Plant, Cell Environ. 37, 1440–1451.
- Meng, T.-T., Wang, H., Harrison, S.P., Prentice, I.C., Ni, J., Wang, G., 2015. Responses of leaf traits to climatic gradients: adaptive variation versus compositional shifts. Biogeosciences 12, 5339–5352.
- Miller, D.M., Bedford, D.R., Hughson, D.L., McDonald, E.V., Robinson, S.E., Schmidt, K.M., 2009. Mapping Mojave Desert ecosystem properties with surficial geology. In: Webb, R.H. (Ed.), The Mojave Desert: Ecosystem Processes and Sustainability. Univ. of Nevada Press, Reno, pp. 225–251.
- Misson, L., Tu, K.P., Boniello, R.A., Goldstein, A.H., 2006. Seasonality of photosynthetic parameters in a multi-specific and vertically complex forest ecosystem in the Sierra Nevada of California. Tree Physiol. 26, 729–741.
- Mohanty, B.P., Skaggs, T.H., 2001. Spatio-temporal evolution and time-stable characteristics of soil moisture within remote sensing footprints with varying soil, slope, and vegetation. Adv. Water Resour. 24, 1051–1067.
- Moles, A.T., Perkins, S.E., Laffan, S.W., et al., 2014. Which is a better predictor of plant traits: temperature or precipitation? J. Veg. Sci. 25, 1167–1180.
- Moradkhani, H., Sorooshian, S., Gupta, H.V., Houser, P.R., 2005. Dual state-parameter estimation of hydrological models using ensemble Kalman filter. Adv. Water Resour. 28, 135–147.
- Muraoka, H., Saigusa, N., Nasahara, K.N., et al., 2010. Effects of seasonal and interannual variations in leaf photosynthesis and canopy leaf area index on gross primary production of a cool-temperate deciduous broadleaf forest in Takayama, Japan. J. Plant. Res. 123, 563–576.
- Myneni, R., Hoffman, S., Knyazikhin, Y., et al., 2002. Global products of vegetation leaf area and fraction absorbed PAR from year one of MODIS data. Remote Sens. Environ. 83, 214–231.
- Nepstad, D.C., de Carvalho, C.R., Davidson, E.A., et al., 1994. The role of deep roots in the hydrological and carbon cycles of Amazonian forests and pastures. Nature 372, 666–669.
- Ng, G., Bedford, D., Miller, D., 2014. A mechanistic modeling and data assimilation framework for Mojave Desert ecohydrology. Water Resour. Res. 4662–4685.
- Ng, G.H.C., Bedford, D.R., Miller, D.M., 2015. Identifying multiple time scale rainfall controls on Mojave Desert ecohydrology using an integrated data and modeling approach for Larrea tridentata. Water Resour. Res. 51, 3884–3899.
- Nielsen, R.L., James, J.J., Drenovsky, R.E., 2019. Functional Traits Explain Variation in Chaparral Shrub Sensitivity to Altered Water and Nutrient Availability. Frontiers. Plant Sci. 10.
- Niinemets, Ü., 1999. Research review. Components of leaf dry mass per area thickness and density – alter leaf photosynthetic capacity in reverse directions in woody plants. New Phytol. 144, 35–47.
- Niinemets, Ü., 2001. Globe scale climatic controls of leaf dry mass per area, density and d thickness in trees and shrubs. Ecology 82, 453–469.
- Niinemets, Ü., 2007. Photosynthesis and resource distribution through plant canopies. Plant, Cell Environ. 30, 1052–1071.
- Nouvellon, Y., Laclau, J.P., Epron, D., et al., 2010. Within-stand and seasonal variations of specific leaf area in a clonal Eucalyptus plantation in the Republic of Congo. For. Ecol. Manage. 259, 1796–1807.
- Oleson, K.W., Bonan, G.B., 2000. The Effects of Remotely Sensed Plant Functional Type and Leaf Area Index on Simulations of Boreal Forest Surface Fluxes by the NCAR Land Surface Model. J. Hydrometeorol. 1, 431–446.
- Oleson KW, Lawrence DM, B G et al. (2010) Technical Description of version 4.0 of the Community Land Model (CLM).
- Oliveira, R.S., Bezerra, L., Davidson, E.A., Pinto, F., Klink, C.A., Nepstad, D.C., Moreir, A., 2005. Deep root function in soil water dynamics in cerrado savannas of central Brazil. Funct. Ecol. 19, 574–581.
- Osnas, J.L.D., Katabuchi, M., Kitajima, K., et al., 2018. Divergent drivers of leaf trait variation within species, among species, and among functional groups. PNAS 115, 5480–5485.
- Oyarzabal, M., Paruelo, J.M., del Pino, F., Oesterheld, M., Lauenroth, W.K., 2008. Trait differences between grass species along a climatic gradient in South and North America. J. Veg. Sci. 19, 183–192.
- Pandey, R.K., Herrera, W.A.T., Villegas, A.N., Pendleton, J.W., 1984. Drought Response of Grain Legumes Under Irrigation Gradient: III. Plant Growth1. Agron. J. 76, 557–560. https://doi.org/10.2134/agronj1984.00021962007600040011x.
- Peguero-Pina, J.J., Sisó, S., Flexas, J., et al., 2017. Cell-level anatomical characteristics explain high mesophyll conductance and photosynthetic capacity in sclerophyllous Mediterranean oaks. New Phytol. 214, 585–596.
- Poorter, H., Niinemets, Ü., Poorter, L., et al., 2009. Causes and consequences of variation in leaf mass per area (LMA):a meta-analysis. New Phytol. 182, 565–588.
- Quero, J.L., Villar, R., Marañón, T., Zamora, R., 2006. Interactions of drought and shade effects on seedlings of four Quercus species: Physiological and structural leaf responses. New Phytol. 170, 819–834.
- Ramírez, D.A., Parra, A., Resco De Dios, V., Moreno, J.M., 2012. Differences in morphophysiological leaf traits reflect the response of growth to drought in a seeder but not in a resprouter Mediterranean species. Funct. Plant Biol. 39, 332–341.
- Raupach, M.R., Rayner, P.J., Barrett, D.J., et al., 2005. Model–data synthesis in terrestrial carbon observation: methods, data requirements and data uncertainty specifications. Glob. Change Biol. 11, 378–397.
- Reich, P.B., Walters, M.B., Ellsworth, D.S., 1991. Leaf age and season influence the relationships between leaf nitrogen, leaf mass per area and photosynthesis in maple and

- oak trees. Plant, Cell Environ. 14, 251-259.
- Reich, P.B., Walters, M.B., Ellsworth, D.S., 1997. From tropics to tundra: Global convergence in plant functioning. In: *Proceedings of the National Academy of Sciences*, 94, 13730 LP –, pp. 13734.
- Reich, P.B., Oleksyn, J., 2004. Global patterns of plant leaf N and P in relation to temperature and latitude. PNAS 101, 11001–11006.
- Reich, P.B., Hobbie, S.E., Lee, T.D., 2014. Plant growth enhancement by elevated CO<sub>2</sub> eliminated by joint water and nitrogen limitation. Nat. Geosci. 7, 920–924.
- Reichle, R.H., McLaughlin, D.B., Entekhabi, D., 2002. Hydrologic data assimilation with the ensemble Kalman filter. Mon. Weather Rev. 130, 103–114.
- Water Resour. Res. 44 (3). https://doi.org/10.1029/2007WR006357.
- Rodriguez-Iturbe, I., D'Odorico, P., Porporato, A., Ridolfi, L., 1999. On the spatial and temporal links between vegetation, climate, and soil moisture. Water Resour. Res. 35, 3709–3722
- Rodriguez-Iturbe, I., 2000. Ecohydrology: A hydrologic perspective of climate-soil-vegetation dynamies. Water Resour. Res. 36, 3–9.
- Rundel, P.W., Gibson, A.C., 2005. Ecological Communities and Processes in a Mojave Desert Ecosystem. Cambridge Univ. Press, N. Y.
- Schenk, H.J., Jackson, R.B., 2002. Rooting depths, lateral root spreads and below-ground/above-ground allometries of plants in water-limited ecosystems. J. Ecol. 90, 480–494.
- Schenk, H.J., Jackson, R.B., 2005. Mapping the global distribution of deep roots in relation to climate and soil characteristics. Geoderma 126, 129–140.
- Schulze, E.D., Turner, N.C., Nicolle, D., Schumacher, J., 2006. Leaf and wood carbon isotope ratios, specific leaf areas and wood growth of Eucalyptus species across a rainfall gradient in Australia. Tree Physiol. 26, 479–492.
- Serbin, S.P., Singh, A., McNeil, B.E., Kingdon, C.C., Townsend, P.A., 2014. Spectroscopic determination of leaf morphological and biochemical traits for northern temperate and boreal tree species. Ecol. Appl. 24, 1651–1669.
- Šímová, I., Violle, C., Svenning, J.C., et al., 2018. Spatial patterns and climate relationships of major plant traits in the New World differ between woody and herbaceous species. J. Biogeogr. 45, 895–916.
- Smirnoff, N., 1998. Plant resistance to environmental stress. Curr. Opin. Biotechnol. 9, 214–219.
- Smith, N.G., Dukes, J.S., 2013. Plant respiration and photosynthesis in global-scale models: incorporating acclimation to temperature and CO<sub>2</sub>. Glob. Change Biol. 19, 45–63.
- Sperry, J.S., Hacke, U.G., 2002. Desert shrub water relations with respect to soil characteristics and plant functional type. Funct. Ecol. 16, 367–378.
- Stephens, G.L., L'Ecuyer, T., Forbroadleaf evergreen shrub R, et al., 2010. Dreary state of precipitation in global models. J. Geophys. Res.: Atmospheres 115.
- Stone, E.L., Kalisz, P.J., 1991. On the maximum extent of tree roots. For. Ecol. Manage. 46, 59-102.
- Sun, Y., Solomon, S., Dai, A., Portmann, R.W., 2006. How Often Does It Rain? J. Clim. 19, 916–934.
- Taylor, K.E., Stouffer, R.J., Meehl, G.A., 2012. An overview of CMIP5 and the experiment design. Bull. Am. Meteorol. Soc. 46, 1–10.
- van Kleunen, M., Fischer, M., 2007. Progress in the detection of costs of phenotypic plasticity in plants. New Phytol. 176, 727–730.
- van Vuuren, D.P., Edmonds, J., Kainuma, M., et al., 2011. The representative concentration pathways: an overview. Clim. Change 109, 5.
- Verheijen, L.M., Brovkin, V., Aerts, R., et al., 2013. Impacts of trait variation through observed trait-climate relationships on performance of an Earth system model: A conceptual analysis. Biogeosciences 10, 5497–5515.
- Verheijen, L.M., Aerts, R., Brovkin, V., Cavender-Bares, J., Cornelissen, J.H.C., Kattge, J., van Bodegom, P.M., 2015. Inclusion of ecologically based trait variation in plant functional types reduces the projected land carbon sink in an earth system model.

- Glob. Change Biol. 21, 3074-3086.
- Wagener, T., Sivapalan, M., Troch, P.A., et al., 2010. The future of hydrology: An evolving science for a changing world. Water Resour. Res. 46, 1–10.
- Wang, Y.-P., Trudinger, C.M., Enting, I.G., 2009. A review of applications of model-data fusion to studies of terrestrial carbon fluxes at different scales. Agric. For. Meteorol. 149, 1829–1842.
- Waring, R.H., Running, S.W., 2010. Forest ecosystems: analysis at multiple scales. Elsevier.
- White, M.A., Thornton, P.E., Running, S.W., Nemani, R.R., 2000. Parameterization and sensitivity analysis of the BIOME-BGC terrestrial ecosystem model: net primary production controls. Earth Interact. 4, 1–85.
- Wieser, G., Oberhuber, W., Waldboth, B., Gruber, A., Matyssek, R., Siegwolf, R.T.W., Grams, T.E.E., 2018. Long-term trends in leaf level gas exchange mirror tree-ring derived intrinsic water-use efficiency of Pinus cembra at treeline during the last century. Agric. For. Meteorol. 248, 251–258.
- Wigmosta, M.S., Vail, L.W., Lettenmaier, D.P., 1994. A distributed hydrology-vegetation model for complex terrain. Water Resour. Res. 30, 1665–1679.
- Williams, M., Schwarz, P.A., Law, B.E., Irvine, J., Kurpius, M.R., 2005. An improved analysis of forest carbon dynamics using data assimilation. Glob. Change Biol. 11, 89–105.
- Williard, K.W.J., Dewalle, D.R., Edwards, P.J., 2005. Influence of bedrock geology and tree species composition on stream nitrate concentrations in mid-Appalachian forested watersheds. Water Air Soil Pollut. 160, 55–76.
- Wilson, K.B., Baldocchi, D.D., Hanson, P.J., 2000. Spatial and seasonal variability of photosynthetic parameters and their relationship to leaf nitrogen in a deciduous forest. Tree Physiol. 20, 565–578.
- Wood, R., 2005. Drizzle in Stratiform Boundary Layer Clouds. Part II: Microphysical Aspects. J. Atmos. Sci. 62, 3034–3050.
- Wright, I.J., Reich, P.B., Westoby, M., 2001. Strategy shifts in leaf physiology, structure and nutrient content between species of high- and low-rainfall and high- and lownutrient habitats. Funct. Ecol. 15, 423–434.
- Wright, I.J., Westoby, M., Reich, P.B., et al., 2004. The worldwide leaf economics spectrum. Nature 428, 821–827.
- Wright, I.J., Reich, P.B., Cornelissen, J.H.C., et al., 2005. Modulation of leaf economic traits and trait relationships by climate. Glob. Ecol. Biogeogr. 14, 411–421.
- Wyant, M.C., Bretherton, C.S., Chlond, A., et al., 2007. A single-column model intercomparison of a heavily drizzling stratocumulus-topped boundary layer. J. Geophys. Res.: Atmospheres 112.
- Xu, L., Baldocchi, D.D., 2003. Seasonal trends in photosynthetic parameters and stomatal conductance of blue oak (Quercus douglasii) under prolonged summer drought and high temperature. Tree Physiol. 23, 865–877.
- Yang, X., Tang, J., Mustard, J.F., Wu, J., Zhao, K., Serbin, S., Lee, J.E., 2016. Seasonal variability of multiple leaf traits captured by leaf spectroscopy at two temperate deciduous forests. Remote Sens. Environ. 179, 1–12.
- Yin, C., Duan, B., Wang, X., Li, C., 2004. Morphological and physiological responses of two contrasting Poplar species to drought stress and exogenous abscisic acid application. Plant Sci. 167, 1091–1097.
- Zadworny, M., McCormack, M.L., Mucha, J., Reich, P.B., Oleksyn, J., 2016. Scots pine fine roots adjust along a 2000-km latitudinal climatic gradient. New Phytol. 212, 389–399.
- Zhang, Y., Chen, J.M., Thomas, S.C., 2007. Retrieving seasonal variation in chlorophyll content of overstory and understory sugar maple leaves from leaf-level hyperspectral data. Can. J. Remote Sens. 33, 406–415.
- Zeng, X., Zeng, X., Barlage, M., 2008. Growing temperate shrubs over arid and semiarid regions in the Community Land Model-Dynamic Global Vegetation Model. Global Biogeochem. Cycles 22, GB3003. https://doi.org/10.1029/2007GB003014.